# Regulation of spindle pole body assembly and cytokinesis by the centrin-binding protein Sfi1 in fission yeast

I-Ju Lee[a,b], Ning Wang[b], Wen Hu[c], Kersey Schott[b], Jürg Bähler[d], Thomas H. Giddings, Jr.[e], John R. Pringle[f], Li-Lin Du[c], and Jian-Qiu Wu[b,g]
[a]Graduate Program of Molecular, Cellular, and Developmental Biology, [b]Department of Molecular Genetics, and [g]Department of Molecular and Cellular Biochemistry, The Ohio State University, Columbus, OH 43210; [c]National Institute of Biological Sciences, Beijing 102206, China; [d]Department of Genetics, Evolution and Environment, University College London, London WC1E 6BT, United Kingdom; [e]Department of Molecular, Cellular, and Developmental Biology, University of Colorado–Boulder, Boulder, CO 80309; [f]Department of Genetics, Stanford University School of Medicine, Stanford, CA 94305

**ABSTRACT** Centrosomes play critical roles in the cell division cycle and ciliogenesis. Sfi1 is a centrin-binding protein conserved from yeast to humans. Budding yeast Sfi1 is essential for the initiation of spindle pole body (SPB; yeast centrosome) duplication. However, the recruitment and partitioning of Sfi1 to centrosomal structures have never been fully investigated in any organism, and the presumed importance of the conserved tryptophans in the internal repeats of Sfi1 remains untested. Here we report that in fission yeast, instead of doubling abruptly at the initiation of SPB duplication and remaining at a constant level thereafter, Sfi1 is gradually recruited to SPBs throughout the cell cycle. Like an *sfi1Δ* mutant, a Trp-to-Arg mutant (*sfi1-M46*) forms monopolar spindles and exhibits mitosis and cytokinesis defects. Sfi1-M46 protein associates preferentially with one of the two daughter SPBs during mitosis, resulting in a failure of new SPB assembly in the SPB receiving insufficient Sfi1. Although all five conserved tryptophans tested are involved in Sfi1 partitioning, the importance of the individual repeats in Sfi1 differs. In summary, our results reveal a link between the conserved tryptophans and Sfi1 partitioning and suggest a revision of the model for SPB assembly.

## INTRODUCTION

Microtubule-organizing centers (MTOCs) are the sites of microtubule nucleation in cells and are essential for the formation of interphase microtubule cytoskeletons, bipolar mitotic spindles, cilia, and flagella. Centrosomes, basal bodies, and their functional equivalents in fungi, spindle pole bodies (SPBs), are the principal MTOCs.

Centrosomes and SPBs are also the hubs of signaling pathways regulating cytokinesis (McCollum and Gould, 2001; Piel *et al.*, 2001; Krapp and Simanis, 2008) and the cell cycle (Pérez-Mongiovi *et al.*, 2000; Doxsey *et al.*, 2005; Hagan, 2008). Owing to the importance of the MTOCs, their duplication and maintenance must be tightly controlled (Nigg and Stearns, 2011), and abnormalities in these structures result in a variety of diseases, including brain development defects, ciliopathies, and cancers (Lingle *et al.*, 1998; Pihan *et al.*, 1998; Fukasawa, 2007; Basto *et al.*, 2008; Ganem *et al.*, 2009; Nigg and Raff, 2009; Bettencourt-Dias *et al.*, 2011).

Centrins are highly conserved, calmodulin-like proteins (Salisbury *et al.*, 1984; Salisbury, 2007; Miron *et al.*, 2011) that are essential for the assembly and integrity of centrosomes, basal bodies, and SPBs in many organisms (Vallen *et al.*, 1994; Middendorp *et al.*, 2000; Salisbury *et al.*, 2002; Paoletti *et al.*, 2003; Stemm-Wolf *et al.*, 2005; Delaval *et al.*, 2011; Dantas *et al.*, 2012; Vonderfecht *et al.*, 2012). Because most centrin molecules are not centrosomal (Paoletti *et al.*, 1996), it is not surprising that centrins also appear to be

involved in other cellular events, including organelle segregation (Selvapandiyan et al., 2007), mRNA transport (Fischer et al., 2004), DNA repair (Araki et al., 2001), and protein degradation (Chen and Madura, 2008). The various functions of centrins are exerted via different binding partners.

Sfi1 (Suppressor of fil1; Ma et al., 1999) is an important binding partner of centrin that has been well characterized in Saccharomyces cerevisiae. Sfi1 contains multiple internal repeats, and each repeat has a conserved Trp (Kilmartin, 2003). Elegant structural analyses showed that in the elongated Sfi1/Cdc31 filament, each Sfi1 repeat binds to one molecule of the centrin Cdc31 (Kilmartin, 2003; Li et al., 2006) and that these proteins colocalize to the half-bridge, the electron-dense region on the nuclear envelope next to the triple-layer core SPB (Byers and Goetsch, 1974; Spang et al., 1993; Adams and Kilmartin, 2000; Kilmartin, 2003; Jaspersen and Winey, 2004). The C-terminus of Sfi1 plays a role in spindle formation (Anderson et al., 2007), but the additional roles of Sfi1 in SPB assembly remain incompletely understood. The elongation of the half-bridge has been hypothesized to be mediated by the interaction between the C-termini of two Sfi1 molecules and to initiate the assembly of the new SPB (Jones and Winey, 2006; Li et al., 2006). However, how and when Sfi1 is recruited to the SPBs remain unknown.

Sfi1 or Sfi1-like proteins have been found in all fungal and animal cells that have been examined, as well as in some more distantly related eukaryotes. It has been postulated that Sfi1 and centrin form the duplication unit that evolved into the cartwheel in centriole duplication (Salisbury, 2007). Strikingly, the ciliate Tetrahymena thermophila has 13 Sfi1-related proteins, which localize asymmetrically on basal bodies (Stemm-Wolf et al., 2013), and in its relative Paramecium tetraurelia, an Sfi1-like protein mediates centrin-based contractility of the cytoskeletal network (Gogendeau et al., 2007). Human hPOC5 has three Sfi1-like centrin-binding repeats and is essential for centriole elongation (Azimzadeh et al., 2009). Another human homologue, hSfi1, also localizes to the centrosomes (Kilmartin, 2003) and interacts with human centrin 2 (Martinez-Sanz et al., 2010), but its function remains unclear.

Of the S. cerevisiae sfi1 or cdc31 mutants identified so far, many arrest with single SPBs and monopolar spindles (Weiss and Winey, 1996; Ivanovska and Rose, 2001; Kilmartin, 2003; Paoletti et al., 2003). Of interest, some temperature-sensitive mutants arrest in the first mitosis after a shift to restrictive temperature, whereas others can form bipolar spindles in the first mitosis and only arrest in the second cell cycle (Ivanovska and Rose, 2001; Kilmartin, 2003). Although monopolar spindle formation is the expected final outcome of a failure in SPB duplication, it has been difficult to explain the differences between these mutants, which will be necessary for full understanding of the functions of centrin and Sfi1. In addition, although the highly conserved Trp in each internal repeat has been presumed to be important for Sfi1 function (Kilmartin, 2003; Li et al., 2006), the consequences of mutations at these sites for function in vivo remain untested.

Whereas the S. cerevisiae SPB is embedded in the nuclear envelope throughout the mitotic cell cycle (Robinow and Marak, 1966; Byers and Goetsch, 1974, 1975), the SPB of the fission yeast Schizosaccharomyces pombe is inserted into the nuclear envelope only during mitosis (McCully and Robinow, 1971; Tanaka and Kanbe, 1986; Ding et al., 1997). During most of the cell cycle, the S. pombe SPB is very close to the cytoplasmic side of the nuclear envelope, similar to centrosomes in metazoans (Bornens, 1977). Thus studying proteins involved in SPB assembly in S. pombe may provide valuable insights into centrosome biology. The morphology of S. pombe SPBs at different cell cycle stages and its mechanisms of duplication have been studied using electron microscopy (EM; McCully and Robinow, 1971; Ding et al., 1997; Uzawa et al., 2004). Duplication appears to initiate in G1/S (Figure 1A), with maturation continuing as the cell cycle proceeds, but this process has been little studied in live cells. S. pombe Sfi1 localizes to SPBs and has 20 internal, Trp-containing repeats, but it shares little homology with S. cerevisiae Sfi1 at the N- and C-termini, and its functions remain largely unknown (Kilmartin, 2003).

Here we describe the first full characterization of Sfi1 in S. pombe. We began with the identification of an sfi1 mutant with cytokinesis phenotypes (sfi1-M46). We found that the mutated residue in Sfi1-M46 is one of the conserved Trps, that the cytokinesis defects are correlated with prolonged septation initiation network (SIN) activity as a consequence of mitotic failure, and that unequal partitioning of Sfi1-M46 underlies the mutant's defects in mitosis and SPB assembly. Strikingly, Sfi1 is recruited to the SPB throughout the cell cycle, suggesting that the current model for SPB assembly may require some modification.

## RESULTS

### A conserved Trp is mutated in the sfi1-M46 mutant

To identify potential regulators of cytokinesis, we examined several uncharacterized morphogenetic mutants that were isolated in a previously described screen (Bähler and Pringle, 1998; Bähler et al., 1998a). Wild-type (wt) S. pombe cells form a single septum perpendicular to the long axis of the cell. In contrast, the M46 mutant exhibited a variety of cytokinesis defects, including long and unseptated cells, cells with multiple and/or aberrant septa, or cell lysis (Figure 1, B and C). In addition, although wt cells form a septum only when they are ~14 μm in length (Martin and Berthelot-Grosjean, 2009; Moseley et al., 2009), many septating M46 cells were <9 μm (Figure 1D). To identify the mutation, the genome of M46 was sequenced, revealing a T-to-C mutation at the sfi1 locus that changes the conserved Trp in the ninth internal repeat to Arg (W434R; Figure 1E). When this same mutation was introduced into a wt strain (see Materials and Methods), the same defects were observed, confirming that the phenotypes observed in M46 are due to the W434R mutation in sfi1. Thus we named the mutant allele sfi1-M46. Because it has never been reported that Sfi1 or Sfi1-like proteins are involved in cytokinesis, we further investigated the functions of Sfi1 and how cytokinesis is affected in sfi1-M46 cells.

### Mitotic defects and aberrant septation in sfi1-M46 cells

In S. pombe, septum formation is regulated by the SPB-associated SIN pathway comprising scaffold proteins, the GTPase Spg1, three kinases, including Cdc7, and their regulators (Krapp and Simanis, 2008; Goyal et al., 2011). We examined SIN activity using a Cdc7–enhanced green fluorescent protein (EGFP) marker, which localizes to SPBs only with GTP-bound Spg1 (Sohrmann et al., 1998; Grallert et al., 2004). In wt cells, GTP-bound Spg1, and thus Cdc7, localizes to both SPBs in early mitosis, but is only on the new SPB beginning in anaphase and begins to disappear during contractile-ring constriction (Goyal et al., 2011; Figure 1F, arrowheads). In contrast, in sfi1-M46 cells, we frequently observed one or more foci of ectopic Cdc7 signal in septated cells (Figure 1F, arrowheads), often accompanied by the assembly of an additional contractile ring and formation of a second septum (Figure 1F). Whether each Cdc7 focus represents one SPB or the SPBs are fragmented in these cells is not clear. Nevertheless, our results suggest that the cytokinesis defects in sfi1-M46 cells are associated with abnormal SIN activity and/or defects in the SPBs.
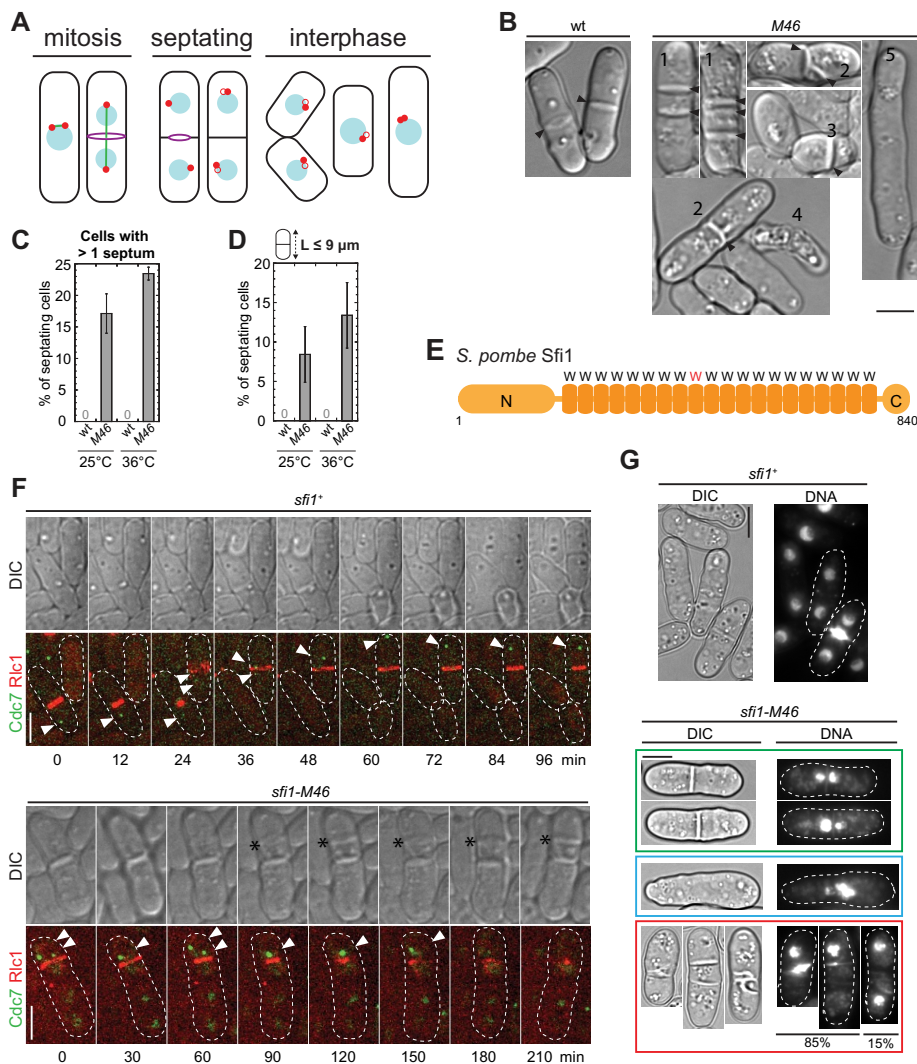
**FIGURE 1:** Mitosis and cytokinesis defects in *sfi1-M46* cells. (A) *S. pombe* cell cycle. Red dots, SPBs; blue circles, nuclei; green line, spindle; purple circles, contractile rings; black, cell wall and septum. Red open circles represent new SPBs that are being assembled; different stages of assembly are not distinguished here. In the rightmost cell, the duplicated SPBs are connected by a bridge before spindle formation and are not resolvable by light microscopy at this stage. (B) DIC images of wt (strain JW729) and *M46* (JW3887) cells grown in YE5S medium at 25°C. The various morphological defects are indicated by numbers: 1) multiple septa; 2) aberrant septa; 3) septum in a short cell; 4) cell lysis; 5) lack of septum in an elongated cell. Arrowheads mark septa. (C, D) Percentages of septating cells with more than one septum (C) and of septating cells <9 μm (D) in wt (JW729) and *M46* (JW3887) cells. Cells were grown in YE5S at 25°C or shifted to 36°C for 4 h before imaging. Means ± SDs from three independent experiments. *n* > 40 septating cells for each experiment. (E) Schematic representation of Sfi1 domains. W, the Trp-containing repeat; the repeat with a mutated Trp in *sfi1-M46* is shown in red. (F) Time courses of localization of Cdc7-EGFP and Rlc1-tdTomato in *sfi1+* (JW4558) or *sfi1-M46* (JW4557) cells. Cdc7 signal is indicated by arrowheads. Asterisks, the abnormal septum. In this and other figures, dashed lines mark cell boundaries. (G) Mitotic defects revealed by Hoechst 33258 staining of *sfi1-M46* cells; the dye stains both DNA and newly formed septa. Green box, cells with one septum and defective DNA separation; blue box, a cell with abnormal DNA but no septum; red box, cells with multiple or abnormal septa. Most such cells also show mitotic defects, but in ~15%, no mitotic defect is evident by DNA staining. Bars, 5 μm.

Mitotic defects were observed in several *S. cerevisiae sfi1* mutants (Kilmartin, 2003; Anderson *et al.*, 2007). Similarly, *S. pombe sfi1-M46* cells also had defects in mitosis. In many cells with or without obvious cytokinesis defects, nuclear DNA was found located exclusively in one of the daughter-cell compartments or stuck in the middle of the cell (Figure 1G), similar to what is observed with the *cut* mutants (Hirano *et al.*, 1986). Thus mitotic defects seem likely to precede the cytokinesis defects in *sfi1-M46* cells, and we focused our further studies on how Sfi1 regulates mitosis and SPB assembly. However, it should be noted that some *sfi1-M46* cells displayed cytokinesis defects without obvious mitosis defects (Figure 1G), so that we cannot rule out the possibility that Sfi1 plays additional direct roles in regulating cytokinesis.

## Sfi1 is essential for bipolar-spindle formation

To test the presumed importance of Sfi1 in mitosis and SPB assembly, we observed the phenotypes of *sfi1Δ* cells. The α-tubulin Atb2 and Pcp1, the homologue of *S. cerevisiae* core SPB protein Spc110 and human pericentrin (Knop and Schiebel, 1997; Flory *et al.*, 2002), were tagged with monomeric red fluorescent protein (mRFP) and GFP to visualize spindles and SPBs, respectively. We generated a diploid strain that was homozygous for the tagged genes and deleted one copy of *sfi1* in this strain. After sporulation, only two spores from each tetrad formed visible colonies (Figure 2A), confirming that *sfi1* is an essential gene, consistent with data from the genome-wide gene-deletion project (Kim *et al.*, 2010). The *sfi1Δ* segregants died as groups of 2–15 cells (Figure 2B). Of interest, tetrad fluorescence microscopy (see *Materials and Methods*) revealed that all four germinated spores from each tetrad formed bipolar spindles in their first mitotic divisions (Figure 2C, *n* = 9 tetrads; Supplemental Video S1). In some tetrads, but not all, monopolar spindles were observed in the *sfi1Δ* colonies during the second mitotic division (Figure 2D, *n* > 10 tetrads; Supplemental Video S2). Thus Sfi1 is essential for bipolar-spindle assembly, although the maternal contribution of Sfi1 is sufficient for successful mitosis at the first cell cycle (and sometimes one or a few additional cell cycles).

## Sfi1 is recruited to SPBs gradually throughout the cell cycle

To further explore Sfi1 function, we tagged the endogenous *sfi1* gene at its C-terminus with sequences encoding tdTomato or monomeric EGFP (mEGFP). Sfi1 localized to SPBs (Figure 3A) as expected (Kilmartin, 2003). However, its colocalization with the pericentrin Pcp1 was not perfect. Before mitotic entry, the Pcp1 focus (containing duplicated but unseparated SPBs) often appeared to be more elongated than the Sfi1 focus (Figure 3B, *t* = −2). In cells entering mitosis, there appeared to be a single Sfi1 focus in the region between the two resolvable Pcp1 foci (Figure 3B, *t* = 0;
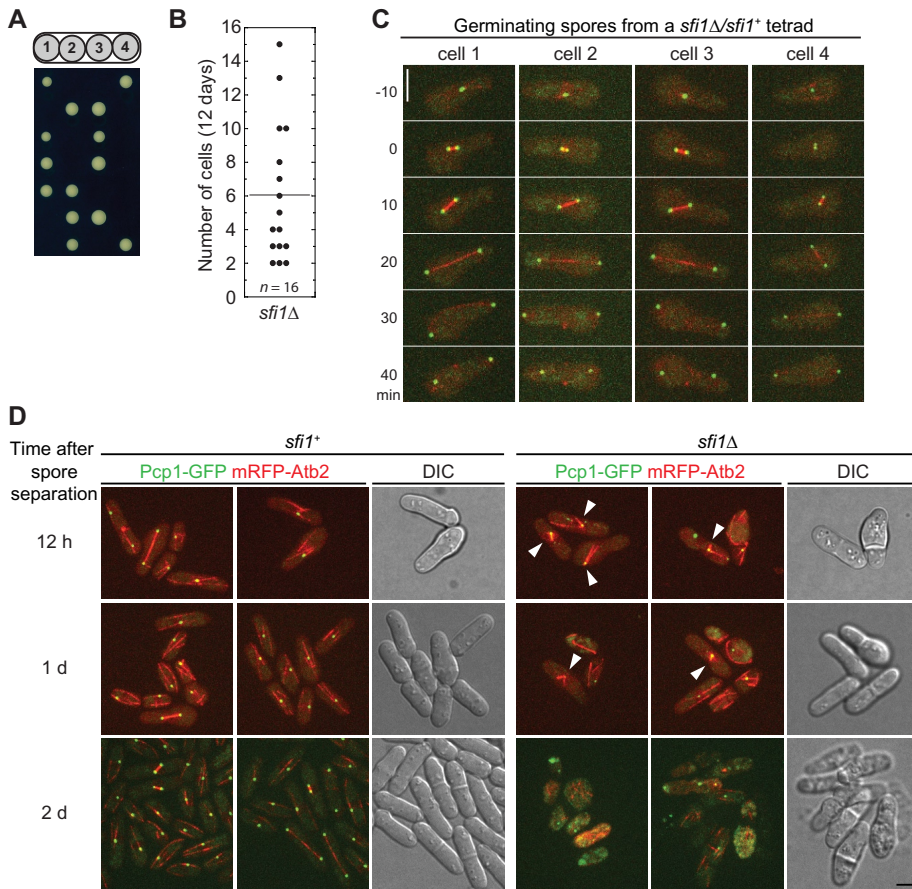
FIGURE 2: Sfi1 is essential for bipolar spindle formation. (A) Dissected tetrads from *sfi1Δ/sfi1+* diploid strain (JW5364) after 7 d on YE5S plate at 25°C. Colonies in each row are from the same tetrad. (B) Cell numbers in *sfi1Δ* microcolonies after tetrads were incubated on YE5S plates at 25°C for 12 d. (C, D) Cells expressing both Pcp1-GFP (green) and mRFP-Atb2 (red). (C) The first mitotic division of the four germinating spores from one *sfi1Δ/sfi1+* tetrad imaged with an interval of 10 min. Time zero indicates SPB separation. See Supplemental Video S1 for the complete time series. (D) Monopolar spindle formation in *sfi1Δ* segregants starting from the second mitotic division. Colonies in the same row are from the same *sfi1Δ/sfi1+* tetrads, and three tetrads imaged at different times are shown. DIC images of one wt and one *sfi1Δ* colony in each tetrad are shown. *sfi1+* colonies at 2 d had grown bigger than the imaged field, so that only the colony edges were imaged. Arrowheads, monopolar spindles. See Supplemental Video S2 for the complete time series. Bars, 5 μm.

*n* = 16 cells). Later, both SPBs had side-by-side Sfi1 and Pcp1 signal (Figure 3B, *t* = 2). We also tested for colocalization of Sfi1 and its presumed binding partner, the centrin Cdc31. As expected, the two proteins colocalized closely (Supplemental Figure S1A). Given these data and previous information about centrins in yeasts (Spang *et al.*, 1993; Paoletti *et al.*, 2003) and Sfi1 in *S. cerevisiae* (Kilmartin, 2003), it seems likely that Sfi1 localizes to the SPB half-bridge in fission yeast.

Using the fluorescence intensity of the SPB-localized SUN-domain protein Sad1-mEGFP as a known standard (Wu and Pollard, 2005), we quantified the numbers of Sfi1-mEGFP molecules in cells and on SPBs. On average, each cell had ~2000 Sfi1 molecules (Supplemental Figure S1B). The total number of Sfi1 molecules increased with cell length, whereas Sfi1 concentration remained constant (Supplemental Figure S1, C and D). Only ~17% of the total Sfi1 molecules were on SPBs (Supplemental Figure S1E). In an asynchronous population, we used the spindle length (distance between the SPBs), septum, and cell length as indicators (Figure 1A) to investigate Sfi1 recruitment to SPBs at different cell cycle stages.

Surprisingly, Sfi1-mEGFP levels on the SPBs increased from 220 ± 60 molecules during septation (*n* = 56) to 360 ± 80 molecules in late G2 (*n* = 23; Figure 3C), which was not predicted by previous models for SPB duplication in budding and fission yeasts (Uzawa *et al.*, 2004; Li *et al.*, 2006). The SPBs in mitotic cells had slightly lower amounts of Sfi1 (190 ± 60 molecules) compared with septating cells (Figure 3C), suggesting that Sfi1 recruitment started during mitosis. To investigate the recruitment of Sfi1 to the SPB with higher temporal resolution, we performed single-cell analysis over time (Figure 3D). Of interest, each daughter SPB inherited less than half of the Sfi1 molecules during SPB separation (~130 at *t* = 0 vs. ~360 at *t* = −10), suggesting that ~100 Sfi1 molecules dissociate from each SPB pair during its separation to form two separate SPBs. Consistent with the observations on the asynchronous population, Sfi1 levels at SPBs gradually increased throughout the cell cycle. Sfi1 was recruited to SPBs at a relatively rapid rate of ~2.4 molecules/min during mitosis (Figure 3D, *t* = 0–30) and at a slower but steady rate of ~0.8 molecule/min during the rest of the cell cycle (Figure 3D, *t* = 30–185), and ~220 Sfi1 molecules were on each SPB during septation (Figure 3D, *t* = 30–55). A concern with using Sfi1-mEGFP to investigate Sfi1 recruitment is that the tagged protein might be recruited differently from the untagged one, particularly given that the C-terminus of Sfi1 is known to be involved in SPB duplication (Li *et al.*, 2006). However, the growth rates of *sfi1-mEGFP* cells were indistinguishable from those of wt cells at both 25 and 36°C (Supplemental Figure S2A). In addition, Sfi1-mEGFP competed efficiently with untagged Sfi1 for localization in diploid cells. We observed Sfi1-mEGFP signal on the SPBs in every *sfi1-mEGFP/sfi1+* diploid cell, just as in haploid or diploid cells expressing only Sfi1-mEGFP (Supplemental Figure S2B and Figure 3A). Moreover, the presence of endogenous untagged Sfi1 reduced Sfi1-mEGFP levels on SPBs to ~50% but did not affect its recruitment pattern, including the faster rate in mitosis and slower rate during the rest of the cell cycle (Supplemental Figure S2C). Thus the mEGFP tag does not appear to significantly affect Sfi1 assembly or function.

The temporal patterns of recruitment of different SPB proteins in live cells have been little studied previously. To test whether what we observed with Sfi1 is a common feature for SPB proteins, we also analyzed the recruitment of four other SPB proteins: Cut12-NEGFP, Pcp1-GFP, Ppc89-GFP, and Sid4-GFP. Cut12 plays a role in inserting SPBs into the nuclear envelope at mitotic entry (Tallada *et al.*, 2009), and the pericentrin Pcp1 recruits the Polo kinase Plo1 and the γ-tubulin complex to SPBs (Fong *et al.*, 2010). Both Cut12-NEGFP and Pcp1-GFP maintained stable levels on SPBs during most of the cell cycle, and their levels increased abruptly right before or during spindle formation (Supplemental Figure S3, A and B). Ppc89 links the SIN pathway to the SPBs (Rosenberg *et al.*, 2006). The Ppc89-GFP
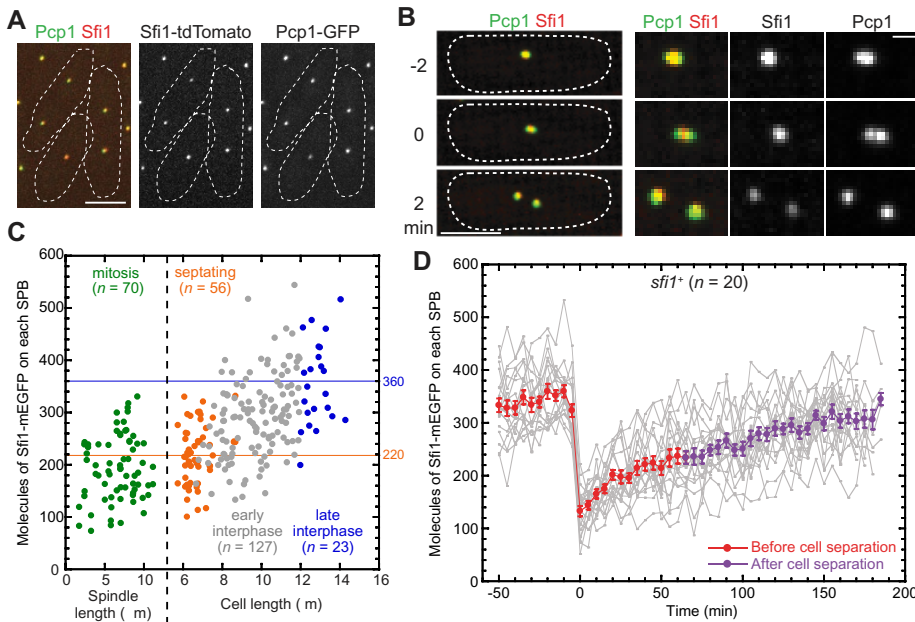
FIGURE 3: Localization and recruitment of Sfi1 to SPBs. (A) Approximate colocalization of Pcp1-GFP and Sfi1-tdTomato (strain JW4685). (B) Spatial relationships between Pcp1-GFP and Sfi1-tdTomato in a cell entering mitosis (JW4685). The first time point with two resolvable Pcp1 foci was defined as time zero. Left, maximum projections of stacks covering the whole cell; right, twofold blow-ups of the images on the left. Bar on the right, 1 µm. (C) Numbers of Sfi1 molecules on each SPB at different cell cycle stages in an asynchronous cell population. For cells in mitosis or septation, each SPB was measured separately for this and other figures. The mean numbers of Sfi1 molecules on each SPB in septating (n = 56) and late interphase (length ≥12 µm; n = 23) cells were 220 and 360, respectively, and are indicated by horizontal lines. (D) Numbers of Sfi1 molecules on SPBs over time in individual wt cells (JW4361). Each gray line represents one SPB. Time zero is the first time point with two resolvable SPBs in that cell. Mean molecules (±SEM) of 20 separated SPBs are plotted in red (before) and purple (after cell separation). Bars, 5 µm (except where noted).

levels on SPBs increased gradually from mitosis to G2, and the recruitment accelerated ~1 h before spindle formation (Supplemental Figure S3C). Sid4 is the scaffold protein for the SIN pathway (Chang and Gould, 2000; Morrell et al., 2004). The Sid4-GFP levels on SPBs increased from late G2 through septation and remained at a steady state during early G2 phase (Supplemental Figure S3D). Thus we found that SPB proteins with different functions had distinct patterns of recruitment during the cell cycle (Supplemental Figure S3E).

## SPB duplication is affected in *sfi1-M46* cells
We next tested whether the mitotic defects in *sfi1-M46* cells might be due to compromised localization of Sfi1 to SPBs. Although 100% of cells expressing Sfi1-mEGFP and Sad1-tdTomato showed colocalization of these proteins at the SPBs, ~28% of cells expressing Sfi1-M46-mEGFP were defective in localizing it to the SPBs (Figure 4A and Supplemental Figure S4A). Moreover, although 100% of wt cells formed bipolar spindles with both Pcp1 and Sfi1 localized to both SPBs (Figure 4, B and D, left), only ~80% of *sfi1-M46* cells formed bipolar spindles (Figure 4B, right, arrowhead). The remaining ~20% of *sfi1-M46* cells formed monopolar spindles (Figure 4B, right, asterisks), and none of these cells showed Sfi1-M46 protein at the SPB (Figure 4C). Even among the *sfi1-M46* cells that formed bipolar spindles, one or both SPBs often failed to show a detectable Sfi1-M46-mEGFP signal (Figure 4D, right). Taken together, these results suggest that Sfi1-M46 does not localize normally to SPBs and that this defect might affect spindle formation.

Fluorescence recovery after photobleaching (FRAP) analyses showed that both Sfi1 and Sfi1-M46 were quite stable on SPBs (Supplemental Figure S4, C and D), and most Sfi1-M46 foci still contained Cdc31 (Supplemental Figure S4E), suggesting that the defects in *sfi1-M46* cells are not due to different Sfi1 dynamics or abolishment of Cdc31 on SPBs. We next quantified the numbers of Sad1 molecules at different cell cycle stages to further investigate the apparent SPBs abnormalities in *sfi1-M46* cells. Like Sfi1, Sad1 on SPBs increased during septation and G2 phase in *sfi1+* and most *sfi1-M46* cells (Supplemental Figure S4, A and B). In wt cells, it increased from ~500 to ~1000 molecules from early mitosis to G2/M (Supplemental Figure S4B). In *sfi1-M46* cells that grew longer without dividing, there were usually ~500 or ~1000 molecules of Sad1 on each SPB (Supplemental Figure S4B), suggesting that Sad1 recruitment and SPB assembly are defective in some *sfi1-M46* cells.

We used EM to further investigate the apparent SPB defects in *sfi1-M46* cells. At the restrictive temperature, 97% of *cdc10-V50* cells arrest with duplicated SPBs connected by the electron-dense bridge (Uzawa et al., 2004). Depending on the angle of sectioning, duplicated SPBs appear as an extended structure in which the central plaques and a well-defined bridge are visible in a single section (Figure 4E) or as an ellipse present in multiple serial sections (Figure 4F). When *sfi1-M46 cdc10-V50* cells were arrested under the same conditions, the morphologies of the SPBs were altered. In some cells, the elliptical electron densities corresponding to the SPBs and bridges appeared in fewer serial sections than in *sfi1+* cells even though the sizes of the ellipses were similar, suggesting that those SPBs had not duplicated (36%, n = 25; Figure 4G). Invagination of the nuclear envelope and the deposition of dark-staining material between it and the SPB are normal features of SPB maturation (Ding et al., 1997; Uzawa et al., 2004). However, in 56% of *sfi1-M46 cdc10-V50* cells with defective SPB duplication (n = 9), dense aggregates were found in the cytoplasm near the SPBs (Figure 4H). These aberrant structures may include components of the cytoplasmic plaques of the SPBs and/or Sfi1-M46 mutant protein and other components of the bridge. In addition, bulges on the nuclear envelope were frequently observed in *sfi1-M46 cdc10-V50* cells (Figure 4H). Although it was not clear from these observations whether the primary defect lies in formation of the half-bridge or in a failure to initiate assembly of the daughter SPB, the data did confirm that SPB assembly is affected in *sfi1-M46* cells.

## Unequal partitioning of Sfi1-M46 during mitosis and its consequences
To explore why SPB assembly is defective in *sfi1-M46* cells, we quantified the Sfi1 and Sad1 levels of the two daughter SPBs in the same cell during mitosis (Figure 5A). In *sfi1+* cells, the two SPBs in one cell had similar amounts of both Sfi1 and Sad1 (Figure 5, A–C). In contrast, in *sfi1-M46* cells, although the relative levels of Sad1 in
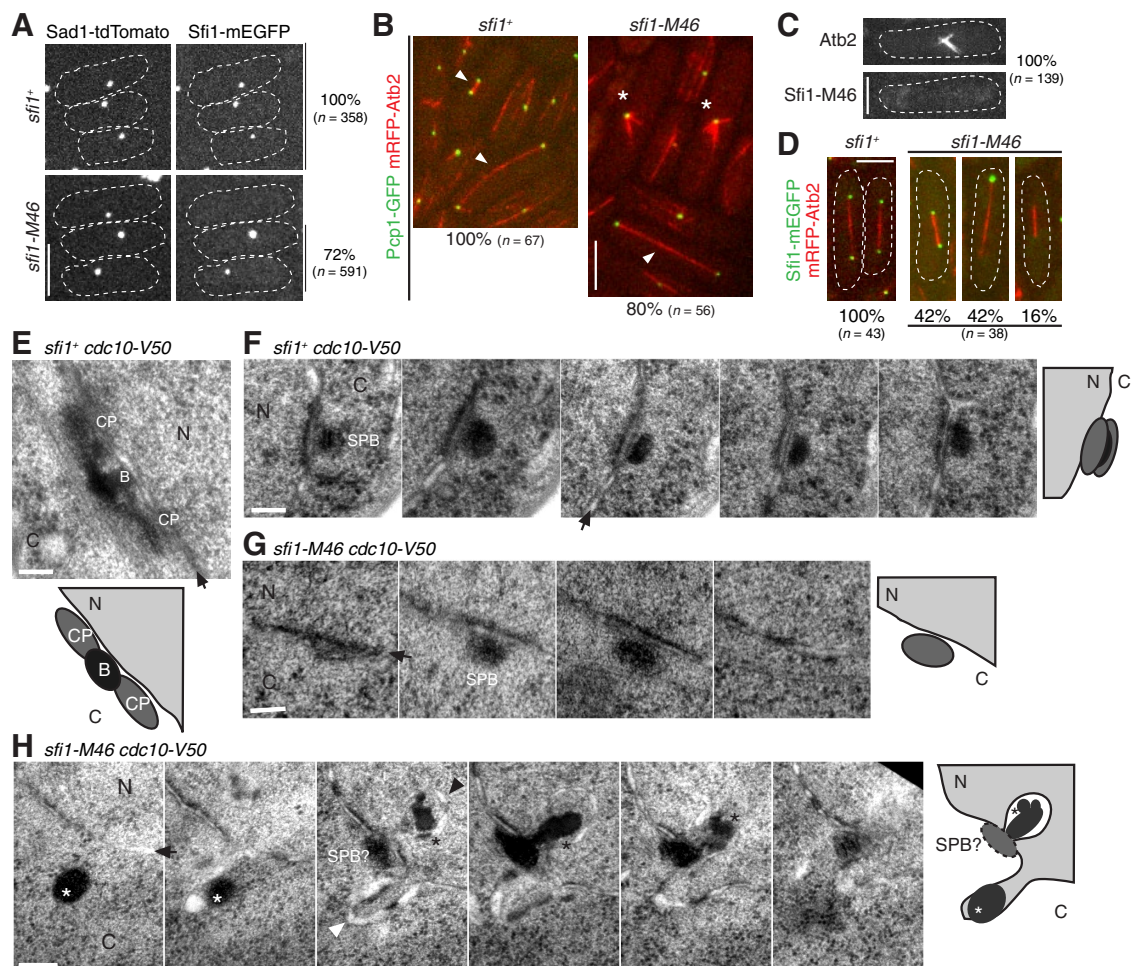
**FIGURE 4:** Regulation of SPB assembly and mitosis by Sfi1. (A) Localization of Sad1 and Sfi1 in *sfi1+* (JW4841) and *sfi1-M46* (JW4842) cells. Percentages of cells with detectable Sfi1-mEGFP signal at the Sad1-tdTomato foci (SPBs) are shown on the right. (B) Monopolar-spindle formation by some *sfi1-M46* cells (asterisks). Arrowheads mark bipolar spindles. Strains were JW5285 and JW5377. The percentages of spindles that were bipolar spindles are shown below the images. (C, D) Localization of Sfi1-mEGFP in *sfi1+* (JW4829) and *sfi1-M46* (JW4831) cells. Spindles are marked by mRFP-Atb2. (C) Apparent absence of Sfi1-M46 from SPBs in cells with monopolar spindles. (D) Absence of detectable Sfi1-M46 at the poles of some bipolar spindles. Percentages of cells with Sfi1-M46 on 2, 1, or 0 SPBs are shown at the bottom. Bars, 5 µm (A–D). (E–H) Electron micrographs of *sfi1+ cdc10-V50* (JW5132; E and F) and *sfi1-M46 cdc10-V50* (JW5130-3; G and H) cells grown at 36°C for 4.5 h. Graphic illustrations are shown below or on the right of micrographs. (F–H) Thin sections spaced at 70 nm of the same cell are shown in each panel. B, the bridge; C, cytoplasm; CP, central plaque, N, nucleus; SPB, spindle pole body. Arrows indicate nuclear envelopes; black arrowhead, invaginated nuclear envelope; white arrowhead, bulged nuclear envelope; black asterisks, dark-stained material deposited close to invaginated nuclear envelope; white asterisks, dark-stained material in the cytoplasm. Bars, 100 nm (E–H).

pairs of SPBs were only slightly altered, the relative levels of Sfi1-M46 could be as different as 100% (Figure 5, B and C; also see Figure 4D), indicating an unequal partitioning of Sfi1 but not Sad1.

We then tested whether Sfi1-M46 localizes preferentially to a specific SPB by comparing the localizations of Sad1, Cdc7, and Sfi1 in *sfi1+* and *sfi1-M46* cells during division. In wt cells, Cdc7 localizes preferentially to the new SPB during late anaphase (Grallert *et al.*, 2004). As expected, 30 min after SPB separation, all *sfi1+* cells had Sad1 and Sfi1 on both SPBs and Cdc7 on one SPB (Figure 5, D and E, pattern I). In contrast, 47% of *sfi1-M46* cells had Sfi1-M46 only on the SPB that lacked Cdc7 (pattern II), 13% had Sfi1-M46 only on the Cdc7-retaining SPB (pattern III), and 4% had no detectable Sfi1-M46 (Figure 5, D and E). We conclude that Sfi1-M46 preferentially remains on the SPB that does not retain Cdc7. This SPB is presumably

the new one, although we cannot exclude the possibility that Cdc7 distribution is affected in *sfi1-M46* cells.

We reasoned that this unequal partitioning of Sfi1-M46 might underlie defects in SPB assembly and spindle formation in the mutant cells that would cause arrest at the second mitosis (Figure 6A). However, the percentage of cells forming monopolar spindles (~20%; Figure 4B) was lower than the percentage of cells presumed to inherit no detectable Sfi1-M46 (34–37%, as calculated from the data in Figures 4D and 5E). These data suggested that the fate of the daughter cell is not solely determined by the inheritance of Sfi1 at mitosis and thus that the recruitment of Sfi1-M46 in interphase might allow some cells to recover enough Sfi1 to assemble a new SPB.

To test this hypothesis, we analyzed the levels of Sfi1 and Sfi1-M46 on SPBs through two cell cycles (Figure 6, B–D). *sfi1+* cells grew
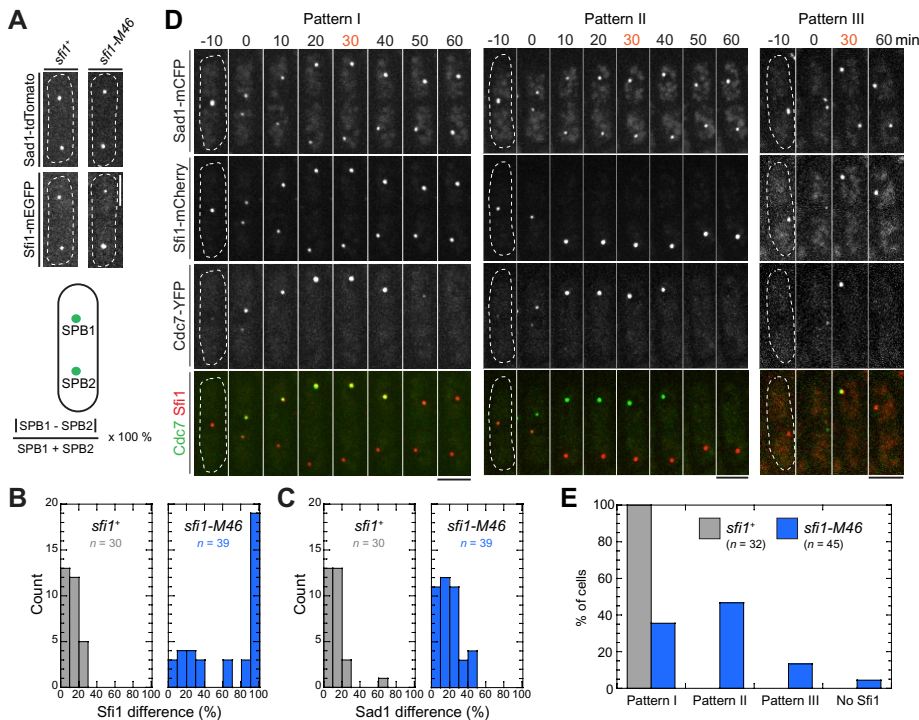
**A**

sfi1⁺  sfi1-M46

Sad1-tdTomato

Sfi1-mEGFP

SPB1

SPB2

$$\frac{|SPB1 - SPB2|}{SPB1 + SPB2} \times 100\%$$

**D**

Pattern I  -10 0 10 20 30 40 50 60

Pattern II  -10 0 10 20 30 40 50 60

Pattern III  -10 0 30 60 min

Sad1-mCFP

Sfi1-mCherry

Cdc7-YFP

Cdc7  Sfi1

**B**

sfi1⁺  n = 30

sfi1-M46  n = 39

Count

Sfi1 difference (%)

**C**

sfi1⁺  n = 30

sfi1-M46  n = 39

Count

Sad1 difference (%)

**E**

sfi1⁺ (n = 32)  sfi1-M46 (n = 45)

% of cells

Pattern I  Pattern II  Pattern III  No Sfi1

**FIGURE 5:** Preferential localization of Sfi1-M46 to the SPB that does not retain Cdc7 during cell division. (A–C) Quantification of fluorescence intensity differences between the two SPBs in individual cells of strains JW4841 (*sfi1⁺*) and JW4842 (*sfi1-M46*). (A) Representative images of Sfi1 and Sad1 and method of calculation. (B, C) Measured differences in Sfi1 (B) and Sad1 (C) intensities. Asynchronous cells with SPBs at a variety of distances from each other were scored. (D, E) Three patterns of Sfi1 partitioning in *sfi1⁺* (JW5203) and *sfi1-M46* (JW5215) cells during division. (D) Images were collected at 10-min intervals; the first time with two distinct Sad1-marked SPBs is set as 0. Pattern I, Sfi1 detectable at both SPBs; pattern II, Sfi1 detectable only at the SPB that does not retain Cdc7 signal; pattern III, Sfi1 detectable only at the SPB that retains Cdc7 signal. Bars, 5 μm. (E) Quantification of cells displaying pattern I, II, or III (or no detectable Sfi1 signal) at the 30-min time point (D).

and divided normally under our long-term imaging conditions (Figure 6C). As expected (Figures 4D and 5B), *sfi1⁺* cells partitioned Sfi1 approximately equally at SPB separation (Figure 6, C and E, and Supplemental Video S3). In contrast, the frequent production of SPBs without detectable Sfi1 in *sfi1-M46* cells (Figures 4, A, C, and D, and 5, B, D, and E) could have either of two sequelae. First, some daughter cells (47% of 43 cells observed) that had no visible Sfi1-M46 signal at mitosis were able to partially recover Sfi1-M46 on the SPB during interphase and form bipolar spindles in the next mitosis (Figure 6, D, 290–360 min, and F(i), and Supplemental Video S4). Second, other cells (53% of the 43 cells) did not recover Sfi1-M46 levels and ended up making unipolar spindles at the next mitosis (Figure 6, D, 420–670 min, and F(ii), and Supplemental Video S4). We also found that unequal partitioning of Sfi1-M46 could occur regardless of its partitioning in the previous cell cycle (Figure 6G). In summary, the unequal partitioning of Sfi1-M46 during SPB separation appears to result in mitotic defects in the next cell cycle, but some cells can recruit sufficient Sfi1-M46 to SPBs in interphase to allow SPB assembly. Consistent with our quantification of Sfi1 levels on SPBs, this result suggests that half-bridge and SPB assembly can start with very limited amounts of Sfi1. It is also possible that half-bridges may undergo de novo assembly.

*sfi1-M46* cells that formed bipolar spindles did not always recover Sfi1-M46 to a high level (Figure 6F). To test whether lower amounts of Sfi1 are sufficient for SPB assembly, we used a

*P81nmt1-mEGFP-sfi1* strain in which the expression of *sfi1* was controlled by the repressible *81nmt1* promoter. Under repressing conditions, the level of Sfi1 on SPBs was ~30% of the endogenous level (Supplemental Figure S5, A and B). *P81nmt1-mEGFP-sfi1* cells appeared normal at 25°C and showed only mild mitosis and cytokinesis defects after 14 h at 36°C (Supplemental Figure S5C). Surprisingly, the number of Sad1 molecules on SPBs in *P81nmt1-mEGFP-sfi1* cells was not distinguishable from that in *sfi1⁺* cells (Supplemental Figure S5D), suggesting that ~30% of normal Sfi1 is sufficient for the assembly of new SPBs.

## Unequal partitioning of Sfi1 in other Trp-to-Arg mutants

The *sfi1-M46* W434R mutation is in the ninth of 20 internal repeats with conserved Trp residues in the *S. pombe* protein. To determine whether it is typical for the centrin-binding Trp to affect the partitioning of Sfi1, we mutated the conserved Trp in the first (W210), sixth (W345), 14th (W573), or 20th (W763) repeat to Arg (Figure 7A). Strains carrying the foregoing mutations were all viable, and all exhibited mitosis and cytokinesis defects similar to that of *sfi1-M46* but to different extents (Figure 7, B and C). At 25°C, the more C-terminal the mutation was, the more severe was the phenotype. However, *sfi1(W210R)* cells were temperature sensitive and formed bipolar spindles at 25°C but monopolar spindles at 36°C (Figure 7, B–D).

We next examined the localization of the mutated Sfi1 proteins. A subset of cells in all four mutants exhibited unequal partitioning of Sfi1 (Figure 7E), suggesting that the conserved Trp residues are indeed important for Sfi1 partitioning. Of interest, localized Sfi1(W763R) was found in many long cells arrested with a single SPB focus (Figure 7E, asterisk), suggesting that the defects in *sfi1(W763R)* cells are not due only to the lack of localized Sfi1(W763R). In summary, although all five of the W-to-R mutants tested have similar phenotypes, it appears that the repeats in Sfi1 are not identical for its function in SPB assembly and spindle formation.

## DISCUSSION
### The model of Sfi1 recruitment and SPB assembly
SPB assembly includes SPB duplication and SPB maturation (Uzawa *et al.*, 2004). In *S. cerevisiae*, the SPB is duplicated by the end of G1 (Byers and Goetsch, 1974, 1975). The bridge between the duplicated SPBs is severed, and a short spindle is formed during late S phase (Lim *et al.*, 2009). The length of the bridge connecting duplicated SPBs and the orientation of the Sfi1 molecules revealed by immuno-EM led to the proposal that half-bridge duplicates by the interaction between C-termini of two Sfi1 molecules to initiate new SPB assembly (Jones and Winey, 2006; Li *et al.*, 2006). In *S. pombe*, it has been proposed that SPB is duplicated at G1/S (Uzawa *et al.*, 2004). However, unduplicated SPBs in a number of wt G2 cells were reported in several studies (Ding *et al.*, 1997; Hoog *et al.*, 2013). It is
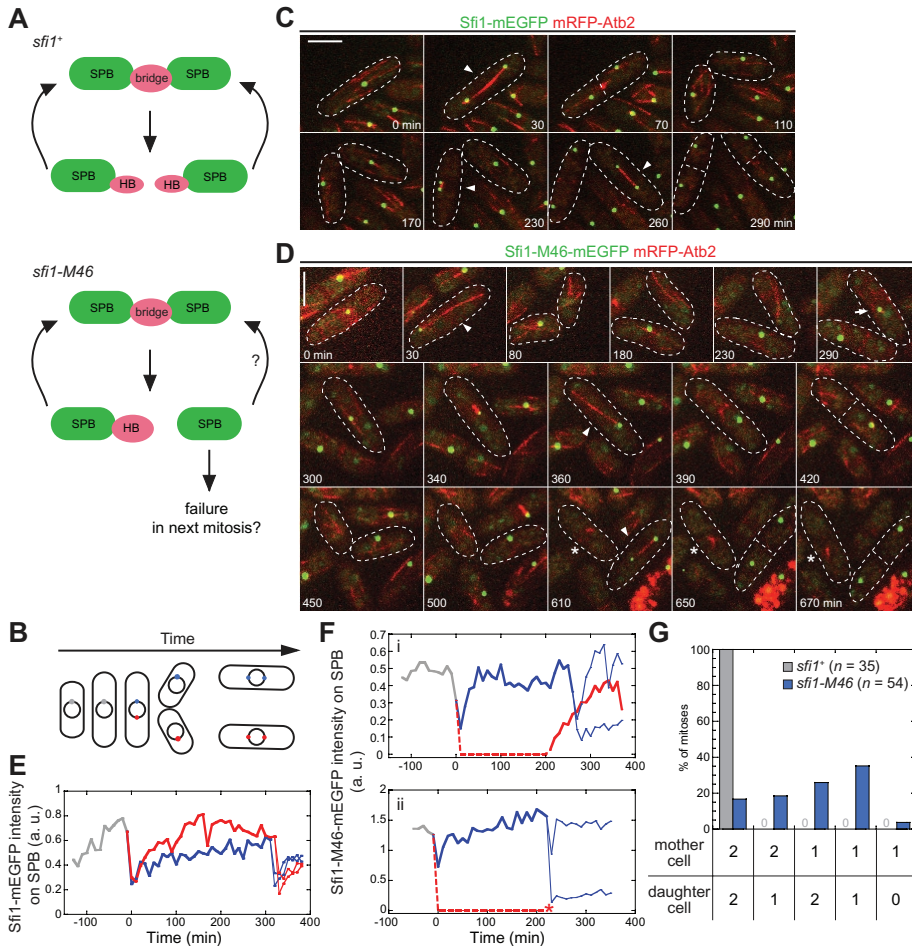
**FIGURE 6:** Unequal partitioning of Sfi1-M46 underlies the mitotic defects. (A) Illustration of SPB-assembly cycle in *sfi1+* and *sfi1-M46* cells (see the text for details). (B) Illustration of imaging cells for two cell cycles. SPB color code as used in E and F. (C, D) Representative images from a time-lapse series with *sfi1+* (C; strain JW4829) and *sfi1-M46* (D; strain JW4831) cells. See Supplemental Videos S3 and S4 for the full series. Arrowheads, bipolar spindles; asterisks, monopolar spindles; arrow, the appearance of Sfi1-M46 in a cell that had no detectable Sfi1 signal on the SPB after the previous mitosis. Bars, 5 µm. (E, F) Sfi1 levels on SPBs through two cell division cycles in *sfi1+* (E) and *sfi1-M46* (F) cells. Time zero is when the first SPB separation occurs. Dashed lines, SPBs without detectable signals at those time points. Asterisk, monopolar spindle formation; a.u., arbitrary units. (G) Quantification of numbers of Sfi1 foci in *sfi1+* and *sfi1-M46* cells during two consecutive mitoses. Daughter cells generated from the first mitosis were analyzed separately in the second mitosis.

*S. cerevisiae* (Jones and Winey, 2006; Li *et al.*, 2006). 2) Sfi1 recruitment may start with the Sfi1-SPB interaction in mitosis, followed by the Sfi1-Sfi1 interaction with slower kinetics (Figure 8; wt, right). The second possibility would predict that unequal Sfi1 partitioning has little effect on SPB assembly, which appears to contradict our results. Alternative to these possibilities, Sfi1-Sfi1 and Sfi1-SPB interactions could take place simultaneously. More work on the kinetics of these interactions is required. In addition, the use of superresolution microscopy and immuno-EM will be important to investigate the exact locations of Sfi1 molecules on SPBs during SPB assembly.

Despite the fact that more work is required to develop a comprehensive model, it is evident that only a limited amount of Sfi1 is required to initiate and complete SPB assembly (Figure 3D and Supplemental Figure S5). The early recruitment of Ppc89 is consistent with its role in localizing other SPB proteins (Rosenberg *et al.*, 2006). The late recruitment of Cut12 and Pcp1 could be due to their accumulation at the new SPB, a possibility that fits with phenotypes of *cut12* and *pcp1* mutants (Tallada *et al.*, 2009; Fong *et al.*, 2010). Taking the results together, we favor a model in which SPB assembly initiates before G1/S and continues in G2 phase, when more Sfi1 molecules are recruited for continuation of SPB assembly and/or SPB maturation (Figure 8). The earlier formation of the spindle in *S. cerevisiae* (during S phase) could make it distinct to *S. pombe* and metazoans (during mitosis) in the timing of centrosome/SPB assembly.

### Sfi1 partition and inheritance
Here we revealed for the first time that the partition of Sfi1 is affected when the conserved tryptophans in internal repeats are mutated (Figures 5–7). The binding of Cdc31 to the mutated repeats might be affected or

possible that the *cdc10-V50* mutant used to synchronize cells at G1/S in Uzawa *et al.* (2004) does not block activities required for SPB duplication, although it prevents cells from entering S phase. Thus investigating Sfi1 recruitment in live cells is critical. Our analyses revealed several unexpected discoveries (Figure 3D): 1) approximately one-third of Sfi1 molecules dissociate from SPBs during SPB separation, which is not observed for other SPB proteins (Supplemental Figure S3); 2) newly separated SPBs recruit Sfi1 with a faster rate during mitosis, and Sfi1 level almost doubles before cell separation (from ~130 to ~220 molecules); and 3) Sfi1 is recruited to SPBs throughout G2 phase at a slower but steady rate.

On the basis of these results and presumed SPB-Sfi1 and Sfi1-Sfi1 interactions, we propose two possibilities to explain Sfi1 recruitment. 1) An extended half-bridge dependent on Sfi1-Sfi1 interaction may be built early, and, as cell cycle progresses, both the old and new SPBs become associated to more Sfi1 molecules (Figure 8; wt, left). This possibility seems to fit better with the EM data in

abolished. The loss of 1 of 20 Cdc31-binding sites might not make a big difference in overall Cdc31 recruitment, as most Sfi1-M46 foci still contain GFP-Cdc31 signal (Supplemental Figure S4E). Instead, the mutations likely affect the structure of the Sfi1-Cdc31 filament. Varied defects in different Trp-to-Arg mutants support this speculation. After unequal partitioning, it is unclear what determines whether SPBs can acquire Sfi1-M46 in interphase. Some SPBs might inherit less but recruit sufficient Sfi1 later, whereas others might associate with little or no Sfi1 and fail SPB assembly (Figure 8). The defective Sfi1 partitioning might result in structural damages on SPBs and prevent half-bridge assembly. Whether any age-dependent modifications contribute to the preference of Sfi1-M46 to the SPB without kinase Cdc7 remains unclear. SPB maturation takes more than one cell cycle, and the NimA kinase Fin1 is a marker for fully matured SPB (Grallert *et al.*, 2004). It will be interesting to investigate whether SPB maturation affects Sfi1 recruitment in different cells.
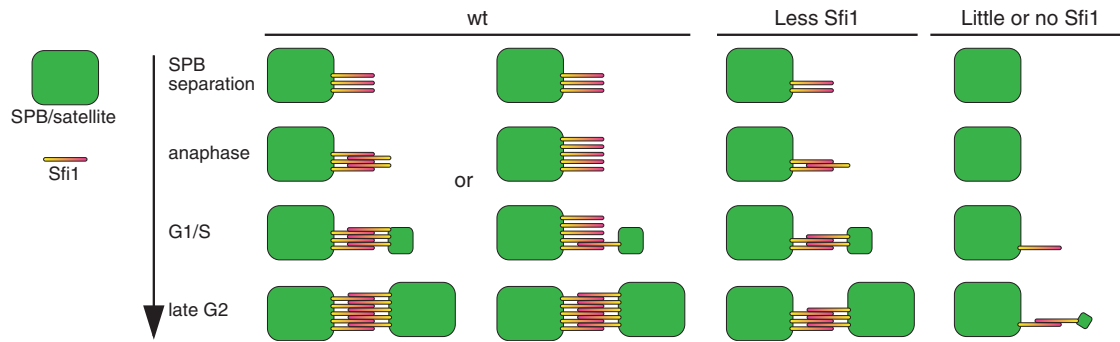
FIGURE 7: The repeats in Sfi1 are all important but are not identical. (A) The positions of the *sfi1* W-to-R mutations examined in this study. (B, C) Phenotypes of the mutant strains (JW5308–JW5311) grown at 25°C or 4 h after a shift to 36°C. (B) DIC and DNA staining; arrowheads, cells with mitosis and/or cytokinesis defects. (C) Quantification of cytokinesis defects as indicated by the presence of more than one septum. Means and SDs from three independent experiments are shown. *n* > 50 septating cells for each experiment. (D) SPBs (Pcp1) and spindles (Atb2) in the mutants (JW5285, JW5379, JW5380, JW5381, and JW5475) at 25 or 36°C. White dashed lines outline mitotic cells; solid white line, a cell apparently without an SPB; arrowheads, bipolar spindles; asterisks, monopolar spindles. (E) Localization of Sad1 and mutant Sfi1 proteins at 25°C (strains JW4841, JW5409, JW5527, JW5410, and JW5474). Arrowheads, SPBs with Sad1 but not Sfi1; asterisk, an elongated cell with a single SPB focus containing Sad1 and Sfi1(W763R). Bars, 5 µm.

During centrosome separation, the connection between two centrosomes must be broken. Centrosome/SPB separation and spindle formation are under the control of CDK and Polo kinase (Lim *et al.*, 1996, 2009; Mayer *et al.*, 1999; Crasta *et al.*, 2008), and the severing of the fibrous linker (Fry *et al.*, 1998; Yang *et al.*, 2002) between two centrosomes is triggered by NimA-related kinase Nek2 (Bahe *et al.*, 2005; Bahmanyar *et al.*, 2008). How the Sfi1-Cdc31 complex reacts to these signals is unknown, but the dissociation of a fraction of Sfi1 molecules (Figure 3D) might be necessary for SPB separation. Many long *sfi1(W763R)* cells arrested with a single SPB focus with localized Sfi1(W763R; Figure 7E), suggesting that, similar to *S. cerevisiae* Sfi1 (Anderson *et al.*, 2007), the C-terminus of *S. pombe* Sfi1 might play additional roles in SPB separation and spindle formation.

## Half-bridge proteins in *S. pombe* and *S. cerevisiae* and their functions

The half-bridge is essential for new SPB assembly (Jaspersen and Winey, 2004). Our results suggest that *S. pombe* Sfi1 also localizes to the half-bridge, although immuno-EM is required for a definitive answer in the future. In addition to Cdc31 and Sfi1, two transmembrane proteins, Kar1 (Rose and Fink, 1987; Spang *et al.*, 1995) and Mps3 (Jaspersen *et al.*, 2002; Nishikawa *et al.*, 2003), also play structural roles in the *S. cerevisiae* half-bridge. In *S. pombe*, no Kar1 homologue has been identified so far. Sad1, a founding member of the SUN protein family (Hagan and Yanagida, 1995), is the presumed homologue of Mps3, and overexpression of Sad1 partially rescued *mps3* phenotypes in *S. cerevisiae* (Jaspersen *et al.*, 2006). It is possible that, like Mps3, Sad1 links the interface of SPB and half-bridge

**FIGURE 8:** Summary of the apparent patterns of Sfi1 recruitment and SPB assembly in wt cells and in mutants that inherit different amounts of Sfi1 at the preceding mitosis.

(Jaspersen *et al.*, 2002) and plays a role in SPB insertion into the nuclear envelope (Araki *et al.*, 2006; Jaspersen *et al.*, 2006; Friederichs *et al.*, 2011).

Centrosome duplication is under the control of Mps1 kinase and Polo-like kinase Plk4 (Winey *et al.*, 1991; Weiss and Winey, 1996; Fisk *et al.*, 2003; Kleylein-Sohn *et al.*, 2007; Peel *et al.*, 2007; Rodrigues-Martins *et al.*, 2007), and Mps1 substrates include centrins (Araki *et al.*, 2010; Yang *et al.*, 2010). Although *S. cerevisiae* half-bridge proteins are all phosphoproteins (Keck *et al.*, 2011) and Sfi1 is a potential substrate of Cdc14 phosphatase (Bloom *et al.*, 2011), a link between phosphorylation of half-bridge proteins and SPB assembly is yet to be established. Mph1, the *S. pombe* Mps1 kinase, does not play a major role in SPB assembly (He *et al.*, 1998). Plo1, the *S. pombe* Polo kinase, localizes to SPBs during mitosis (Mulvihill *et al.*, 1999) and regulates mitotic entry, spindle formation, and cytokinesis (Ohkura *et al.*, 1995; Bähler *et al.*, 1998a; Mulvihill and Hyams, 2002; MacIver *et al.*, 2003; Almonacid *et al.*, 2011; Grallert *et al.*, 2013). How mitotic SPB assembly is affected in *plo1* mutants remains unknown, although Plo1 functions in SPB reorganization during meiosis (Ohta *et al.*, 2012).

### Roles of Sfi1 in cytokinesis

The SPB is the hub of signaling pathways that regulate cytokinesis (Bardin and Amon, 2001; McCollum and Gould, 2001; Pereira and Schiebel, 2001). *S. pombe cdc31* and *sfi1* mutants have similar cytokinesis defects (Figures 1 and 7; Paoletti *et al.*, 2003). Because the asymmetry of SIN signaling is required for normal cytokinesis, it is not surprising that defects in SPB assembly or separation sometimes results in misregulation of SIN activity and the formation of aberrant or additional septa. Although ~15% *sfi1-M46* cells with cytokinesis defects have normal-looking DNA or nuclei (Figure 1G), we have not successfully isolated any separation-of-function *sfi1* mutants. Sfi1-M46 prefers the non–Cdc7-retaining SPB during mitosis, but no obvious correlations were found between the partition of Sfi1 and cytokinesis defects.

In summary, we characterized Sfi1 recruitment throughout the cell cycle, uncovered the importance of the conserved tryptophans for Sfi1 partitioning, and revealed the functional relevance of Sfi1 partition and recruitment. Our study argues that the roles of Sfi1 in centrosome assembly might be more complex than the current model suggests. Further investigation in different model systems is needed to unravel the complexity.

## MATERIALS AND METHODS
### Strain constructions and yeast methods
Table 1 lists the *S. pombe* strains used in this study. Standard growth media and genetic methods were used (Moreno *et al.*, 1991). Media included rich yeast-extract medium plus five supplements (YE5S), Edinburgh minimal medium plus five supplements (EMM5S), and sporulation agar medium plus five supplements (SPA5S). PCR-based gene targeting was performed as described by Bähler *et al.* (1998b). All constructs made in this study were checked by PCR and/or DNA sequencing. Strains with tagged Sfi1 displayed no morphological or cell cycle defects under normal culture conditions and had similar growth rate as wt cells. New mutations in *sfi1* were made using a marker reconstitution mutagenesis method as described previously (Tang *et al.*, 2011), with some modifications. An *sfi1* fragment including the *sfi1* open reading frame (ORF), 70 base pairs of 5′ untranslated region (UTR), and 121 base pairs of 3′ UTR was amplified from genomic DNA and cloned into pH5c, a plasmid with the C-terminus of the *his5* open reading frame and the *kan^R* selectable marker (Tang *et al.*, 2011), using *Bam*HI and *Bgl*II restriction sites included in the primers. Site-directed mutagenesis was then performed as described previously using pairs of back-to-back primers with their 5′ ends adjacent to each other (Lee and Wu, 2012). The first nucleotide (5′) of each forward primer contained the T-to-C mutation that would result in a W-to-R mutation in the Sfi1 protein. Each pair of primers was used to amplify the pH5c-sfi1 plasmid, and ligation of the linear PCR products resulted in plasmids with the desired mutations: pH5c-sfi1(W210R), pH5c-sfi1(W345R), pH5c-sfi1(W434R), pH5c-sfi1(W573R), and pH5c-sfi1(W763R). The mutated *sfi1* fragments were then amplified by PCR and transformed into a strain carrying *sfi1-his5ΔC-kan* (JW4783). *his5+* colonies resulting from marker reconstitution were selected and checked by PCR and sequencing.

Diploid strains were made as described by Moreno *et al.* (1991). To delete the *sfi1* ORF, an *h+/h−* diploid strain homozygous for *pcp1-GFP-kan* and *mRFP-atb2* was transformed with a fragment containing *sfi1Δ::natMX6* with 70 base pairs of sequences homologous to the *sfi1* 5′ and 3′ UTRs. Transformants that grew on YE5S-ade+Nat plates were checked by PCR to confirm the deletion of *sfi1*.

### Whole-genome sequencing to identify the *M46* mutation
About 10⁹ *M46* cells grown on a YE5S plate were harvested, and genomic DNA was extracted using the MasterPure Yeast DNA Purification Kit (Epicentre Biotechnologies, Madison, WI). Genomic DNA was fragmented to the size range of 200–1000 base pairs by sonication. Fragmented DNA was end repaired, dA-tailed using the NEBNext kit (NEB, Ipswich, MA), and ligated to preannealed adaptor oligonucleotides (5′-ACACTCTTTCCCTACACGACGCTCTTC-CGATCTGTAT-3′ and 5′-P-TACAGATCGGAAGAGCGGTTCAG-CAGGAATGCCGAG-3′). Ligation products of 300–500 base pairs were size selected by gel purification and amplified by PCR for

| Strain | Genotype | Source/reference | Strain | Genotype | Source/reference |
|---|---|---|---|---|---|
| JW729 | *h⁺ ade6-M210 leu1-32 ura4-D18* | Wu *et al.* (2003) | JW5308 | *h⁺ sfi1(W210R)-his5⁺-kanMX6 his5Δ ade6-M210 leu1-32 ura4* | This study |
| JW3887 | *h⁺ sfi1-M46 ade6-M216 leu1-32 ura4-D18* | This study | JW5309 | *h⁺ sfi1(W345R)-his5⁺-kanMX6 his5Δ ade6-M210 leu1-32 ura4* | This study |
| JW4361 | *h⁻ sfi1-mEGFP-kanMX6 ade6-M210 leu1-32 ura4-D18* | This study | JW5310 | *h⁺ sfi1(W573R)-his5⁺-kanMX6 his5Δ ade6-M210 leu1-32 ura4* | This study |
| JW4557 | *sfi1-M46 cdc7-EGFP-kanMX6 rlc1-tdTomato-natMX6 ade6 leu1-32 ura4-D18* | This study | JW5311 | *h⁺ sfi1(W763R)-his5⁺-kanMX6 his5Δ ade6-M210 leu1-32 ura4* | This study |
| JW4558 | *h⁺ cdc7-EGFP-kanMX6 rlc1-tdTomato-natMX6 ade6 leu1-32 ura4-D18* | This study | JW5364 | *sfi1Δ::natMX6/sfi1⁺ Patb2-mRFP-atb2/Patb2-mRFP-atb2 pcp1-GFP-kan/pcp1-GFP-kan ade6-M210/ade6-M216 leu1/leu1 ura4/ura4* | This study |
| JW4615 | *h⁻ kanMX6-81nmt1-mEGFP-sfi1 ade6-M210 leu1-32 ura4-D18* | This study | JW5377 | *Patb2-mRFP-atb2 pcp1-GFP-kan sfi1-M46 ade6 leu1-32 ura4-D18* | This study |
| JW4632 | *h⁺ sid4-GFP-kan ade6 leu1 ura4-D18* | This study | JW5379 | *Patb2-mRFP-atb2 pcp1-GFP-kan sfi1(W210R)-his5⁺-kanMX6 ade6-M210 leu1-32 ura4* | This study |
| JW4639 | *h⁺ ppc89-GFP-kan ade6 leu1 ura4* | This study | | | |
| JW4675 | *h⁻ sfi1-tdTomato-natMX6 lys1::nmt1-GFP-cdc31-kan ade6 leu1 ura4* | This study | JW5380 | *Patb2-mRFP-atb2 pcp1-GFP-kan sfi1(W345R)-his5⁺-kanMX6 ade6-M210 leu1-32 ura4* | This study |
| JW4685 | *pcp1-GFP-kan sfi1-tdTomato-natMX6 ade6 leu1 ura4* | This study | JW5381 | *Patb2-mRFP-atb2 pcp1-GFP-kan sfi1(W573R)-his5⁺-kanMX6 ade6-M210 leu1-32 ura4* | This study |
| JW4758 | *lys1::nmt1-GFP-cdc31-kan sfi1-M46-tdTomato-kanMX6 ade6 leu1 ura4* | This study | JW5409 | *sad1-tdTomato-natMX6 sfi1(W210R)-mEGFP-hphMX6 ade6-M210 leu1-32 ura4* | This study |
| JW4783 | *h⁺ sfi1-his5ΔC-kanMX6 his5Δ ade6-M210 leu1-32 ura4* | This study | JW5410 | *sad1-tdTomato-natMX6 sfi1(W573R)-mEGFP-hphMX6 ade6-M210 leu1-32 ura4* | This study |
| JW4829 | *Patb2-mRFP-atb2 sfi1-mEGFP-kanMX6 ade6-M210 leu1-32 ura4-D18* | This study | | | |
| JW4831 | *Patb2-mRFP-atb2 sfi1-M46-mEGFP-kanMX6 ade6 leu1-32 ura4-D18* | This study | JW5474 | *sad1-tdTomato-natMX6 sfi1(W763R)-mEGFP-hphMX6 ade6-M210 leu1-32 ura4* | This study |
| JW4841 | *sad1-tdTomato-natMX6 sfi1-mEGFP-kanMX6 ade6-M210 leu1-32 ura4-D18* | This study | JW5475 | *Patb2-mRFP-atb2 pcp1-GFP-kan sfi1(W763R)-his5⁺-kanMX6 ade6-M210 leu1-32 ura4* | This study |
| JW4842 | *sad1-tdTomato-natMX6 sfi1-M46-mEGFP-kanMX6 ade6 leu1-32 ura4-D18* | This study | | | |
| JW5088 | *sad1-tdTomato-natMX6 kanMX6-81nmt1-mEGFP-sfi1 ade6-M210 leu1-32 ura4-D18* | This study | JW5527 | *sad1-tdTomato-natMX6 sfi1(W345R)-mEGFP-hphMX6 ade6-M210 leu1-32 ura4* | This study |
| JW5130-3 | *cdc10-V50 sfi1-M46-his5⁺-kanMX6 leu1-32 ura4* | This study | JW5933 | *h⁺/h⁻ sfi1⁺/sfi1-mEGFP-kanMX6 ade6-M216/ade6-M210 leu1-32/leu1-32 ura4⁺/ura4-D18* | This study |
| JW5132 | *h⁺ cdc10-V50 ade6-M216 leu1-32 ura4-D18* | This study | | | |
| JW5203 | *sad1-mCFP-kanMX6 cdc7-YFP-kanMX6 sfi1-mCherry-kanMX6 ade6-M210 leu1-32 ura4-D18* | This study | JW5936 | *h⁺/h⁻ sfi1-mEGFP-kanMX6/sfi1-mEGFP-kanMX6 ade6-M216/ade6-M210 leu1-32/leu1-32 ura4⁺/ura4-D18* | This study |
| JW5215 | *sad1-mCFP-kanMX6 cdc7-YFP-kanMX6 sfi1-M46-mCherry-kanMX6 ade6 leu1-32 ura4-D18* | This study | IH1711 | *h⁺ cut12-NEGFP:ura4⁺ leu1-32 ura4-D18* | Iain Hagan (University of Manchester) |
| JW5285 | *h⁻ Patb2-mRFP-atb2 pcp1-GFP-kan ade6-M210 leu1 ura4* | This study | MO1427 | *h⁹⁰ Z2-CFP-atb2-nat lys1::nmt1-GFP-cdc31-kan ade6 leu1 ura4* | Ohta *et al.* (2012) |
| JW5292 | *h⁻ pcp1-GFP-kan ade6-M210 leu1 ura4* | This study | MO1767 | *h⁻ pat1.114 sid4-GFP-kan ade6-M216 leu1* | Ohta *et al.* (2012) |

**TABLE 1:** Fission yeast strains used in this study.

| Strain | Genotype | Source/reference | Strain | Genotype | Source/reference |
|--------|----------|------------------|--------|----------|------------------|
| MO2127 | $h^{90}$ pcp1-GFP-kan hrs1-CFP-nat cut11-mCherry-hph ade6-M216 leu1 ura4 | Ohta et al. (2012) | MS1381 | $h^-$ cut11-3mRFP-hphMX6 leu1-32 ura4-D18 | Sato et al. (2009) |
| MO3501 | $h^{90}$ ppc89-GFP-kan hrs1-CFP-nat cut11-mCherry-hph ade6-M216 leu1 ura4 | Ohta et al. (2012) | SP622 | $h^-$ cdc10-V50 ura4-D18 | Reymond et al. (1992) |
| MS1371 | $h^-$ Patb2-mRFP-atb2 leu1-32 ura4-D18 | Sato et al. (2009) | YS22 | $h^-$ ade5Δ ade7Δ::ade5$^+$ his5Δ ura4-Δ leu1-32 | Tang et al. (2011) |

TABLE 1: Fission yeast strains used in this study. Continued

14 cycles using primers 5'-AATGATACGGCGACCACCGAGATC-TACACTCTTTCCCTACACGACGCTCTTCCGATCT-3' and 5'-CAA-GCAGAAGACGGCATACGAGATCGGTCTCGGCATTCCTGCT-GAACCGCTCTTCCGATCT-3'. The PCR products were purified with the Illustra GFX kit (GE Healthcare, Little Chalfont, UK) and sequenced on an Illumina Hi-Seq 2000 for 49 cycles using the standard sequencing primer. Sequencing read mapping and single nucleotide polymorphism (SNP) calling were carried out using MAQ (Li et al., 2008). Annotation of the SNPs was performed with SnpEff (Cingolani et al., 2012).

## Microscopy and image analysis

Before microscopy, cells were grown in liquid medium (YE5S for haploid strains and YE5S-ade for diploid strains) in exponential phase for ~48 h at 25°C as described by Wu et al. (2006). GFP-cdc31 cells were cultured in YE5S liquid medium for ~24 h, washed in EMM5S medium, and grown in exponential phase in EMM5S for 48 h to induce the expression of GFP-Cdc31. To stain DNA in live cells, cells were washed into EMM5S, and Hoechst 33258 (Sigma-Aldrich, St. Louis, MO) was added to a final concentration of 10 μg/ml from a 1-mg/ml stock. After incubation for 10 min in the dark at room temperature, cells were collected by centrifugation at 5000 rpm for 30 s before imaging.

Microscopy was performed at 23–24°C unless otherwise stated. To image cells at 36°C, cells pregrown at 36°C for appropriate periods were observed on an objective heated with an objective heater (Bioptechs, Butler, PA), and precautions were taken to maintain cells at 36°C throughout sample preparation and image acquisition (Laporte et al., 2011). For most experiments, cells were prepared and imaged using the UltraVIEW ERS spinning-disk confocal microscope (PerkinElmer, Waltham, MA) with a 100×/1.4 numerical aperture Plan-Apo objective lens (Nikon, Melville, NY) as previously described (Coffman et al., 2009; Laporte et al., 2011). Lasers at 488, 514, and 568 nm were used to excite green, yellow, and red fluorescent proteins, respectively. A cooled charge-coupled device (CCD) camera (ORCA-AG; Hamamatsu, Bridgewater, NJ) was used with 2 × 2 binning.

The images in Figures 2, C and D, 3B, 5D, and 6 and Supplemental Figures S1A, S2, and S3 were collected using an equivalent objective on an UltraVIEW Vox CSUX1 spinning-disk confocal microscope (PerkinElmer). Lasers at 440, 488, 515, and 561 nm were used to excite cyan, green, yellow, and red fluorescent proteins, respectively. A back-thinned electron-multiplying CCD camera (Hamamatsu C9100-13) was used without binning. The images shown in Figures 1G and 7B and Supplemental Figure S5C were collected using an equivalent objective on a Nikon Eclipse Ti inverted microscope equipped with differential interference contrast (DIC) and 4',6-diamidino-2-phenylindole filters and a Nikon DS-QI1 cooled CCD camera. In experiments that required imaging of the same cells over a long period of time, 2 μl of concentrated cells from an exponential-phase liquid culture (OD$_{590}$ 0.2–0.5) were placed in a 35-mm dish with a glass coverslip bottom (0420041500C; Bioptechs) and covered with a piece of YE5S agar.

For tetrad fluorescence microscopy, diploid cells were streaked onto an SPA5S plate and incubated at 25°C for 1–3 d. After picking tetrads and separating spores on a YE5S plate using a tetrad-dissection microscope, cells were incubated at 25°C for 0.5–2 d. Then a piece of YE5S agar with the cells to be imaged was cut out from the plate and inverted onto a 60 mm × 24 mm coverslip (Fisher-Brand 22266882). The positions of colonies on the automated stage of the UltraVIEW Vox CSUX1 system were identified and saved, and cells at these positions were imaged at every time point using Volocity software.

The images in figures are maximum-intensity projections of z-sections spaced at 0.2–0.6 μm except where noted. Merged images of two channels were generated using UltraVIEW, Volocity, or ImageJ.

## Quantification of protein molecules

Fluorescence intensities were quantified as described previously (Wu and Pollard, 2005; Wu et al., 2008; Laporte et al., 2011) with some modifications. For measuring fluorescence intensities of SPB proteins, the focal plane with the maximum intensity (Figure 3C and Supplemental Figures S4, A and B, and S5, B and D) or the summed intensities of z-sections spaced at 0.4 μm for each SPB (Figure 3D and Supplemental Figures S2C and S3) were used. When Sfi1-mEGFP was quantified with both methods, the results were statistically indistinguishable from each other, suggesting that it does not make a significant difference in this application because all of the quantified proteins are in the same structure. The florescence intensity in a 6 × 6–pixel region of interest (ROI) was measured, and a concentric 10 × 10–pixel ROI was used to correct for the cellular background. To convert fluorescence intensities to numbers of molecules, cells expressing Sad1-mEGFP or Sad1-tdTomato in early mitosis (distance between the two SPBs <2 μm) were used as standards, and the mean number of Sad1 molecules in each SPB ($n > 20$) was set at 500 (Wu and Pollard, 2005). Recruitment rates of Sfi1-mEGFP in mitosis and interphase were slopes of the linear curve fits for 0–30 and 30–185 min after SPB separation, respectively.

To calculate the concentration of Sfi1 in the whole cell during interphase or septation (Supplemental Figure S1D), cell area ($A$) was measured and converted to cell volume as described previously (Wu and Pollard, 2005; Wu et al., 2008). To compare the number of molecules on SPBs in early versus late G2 in an unsynchronized culture, we also converted the measured cell area to cell length as follows. The two-dimensional shape of a fission yeast cell was assumed to be

a rectangle capped by a semicircle at each end, and the cell width, and thus the diameter of the circle, was taken as 4 µm. Therefore, if cell length is L micrometers, A measured is equal to the area of the rectangle, $(L-4) \times 4$, plus the area of the two semicircles, $[(\pi \times 4)/2] \times 2$. Therefore cell area can be converted to cell length using the equation $L = A/4 - \pi + 4$. For cells with two SPBs and no septum (mitotic cells), the three-dimensional distance (D) between two SPBs was calculated using the equation $D^2 = d_{xy}^2 + d_z^2$ and taken as the spindle length. The distance $d_{xy}$ between two SPBs was measured by drawing a line connecting two SPBs in maximum-intensity projection, and the distance $d_z$ was the spacing in the z-axis between the best focal planes for the two SPBs.

## FRAP analysis

FRAP analysis was performed using the photokinesis unit on the UltraVIEW ERS confocal system. A picture at the middle of a group of cells was taken first, and several $6 \times 6$–pixel ROIs were drawn at sites with the best-focused Sfi1 signals in the same focal plane. Fluorescence in the ROIs was bleached after four prebleach images were collected, and then 120 postbleach images were collected at 2-s intervals. Data analyses were performed as described by Coffman *et al.* (2009), with corrections of background and photobleaching during image acquisition. SPBs that moved out of the focal plane during image acquisition were excluded from the analyses. Percentage recovery was plotted using KaleidaGraph. Kymographs were produced using ImageJ, and the plug-in SpeckleTrackerJ (http://athena.physics.lehigh.edu/speckletrackerj/index.chy) from Dimitrios Vavylonis's group was used to center the position of each SPB.

## Electron microscopy

To synchronize cells at G1/S, strains JW5132 (*sfi1⁺ cdc10-V50*) and JW5130-3 (*sfi1-M46 cdc10-V50*) were cultured at 25°C for 2 d in exponential phase and shifted to 36°C for 4.5 h. Cells were harvested at 36°C and prepared for EM as described previously (Giddings *et al.*, 2001). Briefly, cells were harvested on Millipore filters and frozen in a Wohlwend Compact 02 High Pressure Freezer. The cryofixed cells were freeze substituted in the presence of 2% osmium tetroxide and 0.1% uranyl acetate in acetone and then embedded in Epon-Araldite epoxy resin. Blocks of embedded cells were serially sectioned at a thickness of 70 nm and poststained with uranyl acetate and lead citrate. Sections were then observed on a Philips CM100 transmission electron microscope (FEI, Hillsboro, OR).

## REFERENCES

Adams IR, Kilmartin JV (2000). Spindle pole body duplication: a model for centrosome duplication? Trends Cell Biol 10, 329–335.

Almonacid M, Celton-Morizur S, Jakubowski JL, Dingli F, Loew D, Mayeux A, Chen JS, Gould KL, Clifford DM, Paoletti A (2011). Temporal control of contractile ring assembly by Plo1 regulation of myosin II recruitment by Mid1/anillin. Curr Biol 21, 473–479.

Anderson VE, Prudden J, Prochnik S, Giddings TH Jr, Hardwick KG (2007). Novel *sfi1* alleles uncover additional functions for Sfi1p in bipolar spindle assembly and function. Mol Biol Cell 18, 2047–2056.

Araki Y, Gombos L, Migueleti SP, Sivashanmugam L, Antony C, Schiebel E (2010). N-terminal regions of Mps1 kinase determine functional bifurcation. J Cell Biol 189, 41–56.

Araki Y, Lau CK, Maekawa H, Jaspersen SL, Giddings TH Jr, Schiebel E, Winey M (2006). The *Saccharomyces cerevisiae* spindle pole body (SPB) component Nbp1p is required for SPB membrane insertion and interacts with the integral membrane proteins Ndc1p and Mps2p. Mol Biol Cell 17, 1959–1970.

Araki M, Masutani C, Takemura M, Uchida A, Sugasawa K, Kondoh J, Ohkuma Y, Hanaoka F (2001). Centrosome protein centrin 2/caltractin 1 is part of the xeroderma pigmentosum group C complex that initiates global genome nucleotide excision repair. J Biol Chem 276, 18665–18672.

Azimzadeh J, Hergert P, Delouvee A, Euteneuer U, Formstecher E, Khodjakov A, Bornens M (2009). hPOC5 is a centrin-binding protein required for assembly of full-length centrioles. J Cell Biol 185, 101–114.

Bahe S, Stierhof YD, Wilkinson CJ, Leiss F, Nigg EA (2005). Rootletin forms centriole-associated filaments and functions in centrosome cohesion. J Cell Biol 171, 27–33.

Bähler J, Pringle JR (1998). Pom1p, a fission yeast protein kinase that provides positional information for both polarized growth and cytokinesis. Genes Dev 12, 1356–1370.

Bähler J, Steever AB, Wheatley S, Wang Y-L, Pringle JR, Gould KL, McCollum D (1998a). Role of polo kinase and Mid1p in determining the site of cell division in fission yeast. J Cell Biol 143, 1603–1616.

Bähler J, Wu J-Q, Longtine MS, Shah NG, McKenzie A III, Steever AB, Wach A, Philippsen P, Pringle JR (1998b). Heterologous modules for efficient and versatile PCR-based gene targeting in *Schizosaccharomyces pombe*. Yeast 14, 943–951.

Bahmanyar S, Kaplan DD, Deluca JG, Giddings TH Jr, O'Toole ET, Winey M, Salmon ED, Casey PJ, Nelson WJ, Barth AI (2008). β-Catenin is a Nek2 substrate involved in centrosome separation. Genes Dev 22, 91–105.

Bardin AJ, Amon A (2001). MEN and SIN: what's the difference? Nat Rev Mol Cell Biol 2, 815–826.

Basto R, Brunk K, Vinadogrova T, Peel N, Franz A, Khodjakov A, Raff JW (2008). Centrosome amplification can initiate tumorigenesis in flies. Cell 133, 1032–1042.

Bettencourt-Dias M, Hildebrandt F, Pellman D, Woods G, Godinho SA (2011). Centrosomes and cilia in human disease. Trends Genet 27, 307–315.

Bloom J, Cristea IM, Procko AL, Lubkov V, Chait BT, Snyder M, Cross FR (2011). Global analysis of Cdc14 phosphatase reveals diverse roles in mitotic processes. J Biol Chem 286, 5434–5445.

Bornens M (1977). Is the centriole bound to the nuclear membrane? Nature 270, 80–82.

Byers B, Goetsch L (1974). Duplication of spindle plaques and integration of the yeast cell cycle. Cold Spring Harb Symp Quant Biol 38, 123–131.

Byers B, Goetsch L (1975). Behavior of spindles and spindle plaques in the cell cycle and conjugation of *Saccharomyces cerevisiae*. J Bacteriol 124, 511–523.

Chang L, Gould KL (2000). Sid4p is required to localize components of the septation initiation pathway to the spindle pole body in fission yeast. Proc Natl Acad Sci USA 97, 5249–5254.

Chen L, Madura K (2008). Centrin/Cdc31 is a novel regulator of protein degradation. Mol Cell Biol 28, 1829–1840.

Cingolani P, Platts A, Wang L, Coon M, Nguyen T, Wang L, Land SJ, Lu X, Ruden DM (2012). A program for annotating and predicting the effects of single nucleotide polymorphisms, SnpEff: SNPs in the genome of *Drosophila melanogaster* strain w1118; iso-2; iso-3. Fly 6, 80–92.

Coffman VC, Nile AH, Lee I-J, Liu H, Wu J-Q (2009). Roles of formin nodes and myosin motor activity in Mid1p-dependent contractile-ring assembly during fission yeast cytokinesis. Mol Biol Cell 20, 5195–5210.

Crasta K, Lim HH, Giddings TH Jr, Winey M, Surana U (2008). Inactivation of Cdh1 by synergistic action of Cdk1 and polo kinase is necessary for proper assembly of the mitotic spindle. Nat Cell Biol 10, 665–675.

Dantas TJ, Daly OM, Morrison CG (2012). Such small hands: the roles of centrins/caltractins in the centriole and in genome maintenance. Cell Mol Life Sci 69, 2979–2997.

Delaval B, Covassin L, Lawson ND, Doxsey S (2011). Centrin depletion causes cyst formation and other ciliopathy-related phenotypes in zebrafish. Cell Cycle 10, 3964–3972.

Ding R, West RR, Morphew DM, Oakley BR, McIntosh JR (1997). The spindle pole body of *Schizosaccharomyces pombe* enters and leaves the nuclear envelope as the cell cycle proceeds. Mol Biol Cell 8, 1461–1479.

Doxsey S, McCollum D, Theurkauf W (2005). Centrosomes in cellular regulation. Annu Rev Cell Dev Biol 21, 411–434.

Fischer T, Rodriguez-Navarro S, Pereira G, Racz A, Schiebel E, Hurt E (2004). Yeast centrin Cdc31 is linked to the nuclear mRNA export machinery. Nat Cell Biol 6, 840–848.

Fisk HA, Mattison CP, Winey M (2003). Human Mps1 protein kinase is required for centrosome duplication and normal mitotic progression. Proc Natl Acad Sci USA 100, 14875–14880.

Flory MR, Morphew M, Joseph JD, Means AR, Davis TN (2002). Pcp1p, an Spc110p-related calmodulin target at the centrosome of the fission yeast Schizosaccharomyces pombe. Cell Growth Differ 13, 47–58.

Fong CS, Sato M, Toda T (2010). Fission yeast Pcp1 links polo kinase-mediated mitotic entry to γ-tubulin-dependent spindle formation. EMBO J 29, 120–130.

Friederichs JM, Ghosh S, Smoyer CJ, McCroskey S, Miller BD, Weaver KJ, Delventhal KM, Unruh J, Slaughter BD, Jaspersen SL (2011). The SUN protein Mps3 is required for spindle pole body insertion into the nuclear membrane and nuclear envelope homeostasis. PLoS Genet 7, e1002365.

Fry AM, Mayor T, Meraldi P, Stierhof YD, Tanaka K, Nigg EA (1998). C-Nap1, a novel centrosomal coiled-coil protein and candidate substrate of the cell cycle-regulated protein kinase Nek2. J Cell Biol 141, 1563–1574.

Fukasawa K (2007). Oncogenes and tumour suppressors take on centrosomes. Nat Rev Cancer 7, 911–924.

Ganem NJ, Godinho SA, Pellman D (2009). A mechanism linking extra centrosomes to chromosomal instability. Nature 460, 278–282.

Giddings TH Jr, O'Toole ET, Morphew M, Mastronade DN, McIntosh JR, Winey M (2001). Using rapid freeze and freeze-substitution for the preparation of yeast cells for electron microscopy and three-dimensional analysis. Methods Cell Biol 67, 27–42.

Gogendeau D, Beisson J, de Loubresse NG, Le Caer JP, Ruiz F, Cohen J, Sperling L, Koll F, Klotz C (2007). An Sfi1p-like centrin-binding protein mediates centrin-based Ca$^{2+}$-dependent contractility in Paramecium tetraurelia. Eukaryot Cell 6, 1992–2000.

Goyal A, Takaine M, Simanis V, Nakano K (2011). Dividing the spoils of growth and the cell cycle: the fission yeast as a model for the study of cytokinesis. Cytoskeleton (Hoboken) 68, 69–88.

Grallert A, Krapp A, Bagley S, Simanis V, Hagan IM (2004). Recruitment of NIMA kinase shows that maturation of the S. pombe spindle-pole body occurs over consecutive cell cycles and reveals a role for NIMA in modulating SIN activity. Genes Dev 18, 1007–1021.

Grallert A, Patel A, Tallada VA, Chan KY, Bagley S, Krapp A, Simanis V, Hagan IM (2013). Centrosomal MPF triggers the mitotic and morphogenetic switches of fission yeast. Nat Cell Biol 15, 88–95.

Hagan IM (2008). The spindle pole body plays a key role in controlling mitotic commitment in the fission yeast Schizosaccharomyces pombe. Biochem Soc Trans 36, 1097–1101.

Hagan I, Yanagida M (1995). The product of the spindle formation gene sad1+ associates with the fission yeast spindle pole body and is essential for viability. J Cell Biol 129, 1033–1047.

He X, Jones MH, Winey M, Sazer S (1998). Mph1, a member of the Mps1-like family of dual specificity protein kinases, is required for the spindle checkpoint in S. pombe. J Cell Sci 111, 1635–1647.

Hirano T, Funahashi S, Uemura T, Yanagida M (1986). Isolation and characterization of Schizosaccharomyces pombe cut mutants that block nuclear division but not cytokinesis. EMBO J 5, 2973–2979.

Hoog JL, Huisman SM, Brunner D, Antony C (2013). Electron tomography reveals novel microtubule lattice and microtubule organizing centre defects in +TIP mutants. PloS One 8, e61698.

Ivanovska I, Rose MD (2001). Fine structure analysis of the yeast centrin, Cdc31p, identifies residues specific for cell morphology and spindle pole body duplication. Genetics 157, 503–518.

Jaspersen SL, Giddings TH Jr, Winey M (2002). Mps3p is a novel component of the yeast spindle pole body that interacts with the yeast centrin homologue Cdc31p. J Cell Biol 159, 945–956.

Jaspersen SL, Martin AE, Glazko G, Giddings TH Jr, Morgan G, Mushegian A, Winey M (2006). The Sad1-UNC-84 homology domain in Mps3 interacts with Mps2 to connect the spindle pole body with the nuclear envelope. J Cell Biol 174, 665–675.

Jaspersen SL, Winey M (2004). The budding yeast spindle pole body: structure, duplication, and function. Annu Rev Cell Dev Biol 20, 1–28.

Jones MH, Winey M (2006). Centrosome duplication: is asymmetry the clue? Curr Biol 16, R808-R810.

Keck JM, Jones MH, Wong CC, Binkley J, Chen D, Jaspersen SL, Holinger EP, Xu T, Niepel M, Rout MP, et al. (2011). A cell cycle phosphoproteome of the yeast centrosome. Science 332, 1557–1561.

Kilmartin JV (2003). Sfi1p has conserved centrin-binding sites and an essential function in budding yeast spindle pole body duplication. J Cell Biol 162, 1211–1221.

Kim DU, Hayles J, Kim D, Wood V, Park HO, Won M, Yoo HS, Duhig T, Nam M, Palmer G, et al. (2010). Analysis of a genome-wide set of gene deletions in the fission yeast Schizosaccharomyces pombe. Nat Biotechnol 28, 617–623.

Kleylein-Sohn J, Westendorf J, Le Clech M, Habedanck R, Stierhof YD, Nigg EA (2007). Plk4-induced centriole biogenesis in human cells. Dev Cell 13, 190–202.

Knop M, Schiebel E (1997). Spc98p and Spc97p of the yeast g-tubulin complex mediate binding to the spindle pole body via their interaction with Spc110p. EMBO J 16, 6985–6995.

Krapp A, Simanis V (2008). An overview of the fission yeast septation initiation network (SIN). Biochem Soc Trans 36, 411–415.

Laporte D, Coffman VC, Lee I-J, Wu J-Q (2011). Assembly and architecture of precursor nodes during fission yeast cytokinesis. J Cell Biol 192, 1005–1021.

Lee I-J, Wu J-Q (2012). Characterization of Mid1 domains for targeting and scaffolding in fission yeast cytokinesis. J Cell Sci 125, 2973–2985.

Li H, Ruan J, Durbin R (2008). Mapping short DNA sequencing reads and calling variants using mapping quality scores. Genome Res 18, 1851–1858.

Li S, Sandercock AM, Conduit P, Robinson CV, Williams RL, Kilmartin JV (2006). Structural role of Sfi1p-centrin filaments in budding yeast spindle pole body duplication. J Cell Biol 173, 867–877.

Lim HH, Goh PY, Surana U (1996). Spindle pole body separation in Saccharomyces cerevisiae requires dephosphorylation of the tyrosine 19 residue of Cdc28. Mol Cell Biol 16, 6385–6397.

Lim HH, Zhang T, Surana U (2009). Regulation of centrosome separation in yeast and vertebrates: common threads. Trends Cell Biol 19, 325–333.

Lingle WL, Lutz WH, Ingle JN, Maihle NJ, Salisbury JL (1998). Centrosome hypertrophy in human breast tumors: implications for genomic stability and cell polarity. Proc Natl Acad Sci USA 95, 2950–2955.

Ma P, Winderickx J, Nauwelaers D, Dumortier F, De Doncker A, Thevelein JM, Van Dijck P (1999). Deletion of SFI1, a novel suppressor of partial Ras-cAMP pathway deficiency in the yeast Saccharomyces cerevisiae, causes G$_2$ arrest. Yeast 15, 1097–1109.

MacIver FH, Tanaka K, Robertson AM, Hagan IM (2003). Physical and functional interactions between polo kinase and the spindle pole component Cut12 regulate mitotic commitment in S. pombe. Genes Dev 17, 1507–1523.

Martin SG, Berthelot-Grosjean M (2009). Polar gradients of the DYRK-family kinase Pom1 couple cell length with the cell cycle. Nature 459, 852–856.

Martinez-Sanz J, Kateb F, Assairi L, Blouquit Y, Bodenhausen G, Abergel D, Mouawad L, Craescu CT (2010). Structure, dynamics and thermodynamics of the human centrin 2/hSfi1 complex. J Mol Biol 395, 191–204.

Mayer TU, Kapoor TM, Haggarty SJ, King RW, Schreiber SL, Mitchison TJ (1999). Small molecule inhibitor of mitotic spindle bipolarity identified in a phenotype-based screen. Science 286, 971–974.

McCollum D, Gould KL (2001). Timing is everything: regulation of mitotic exit and cytokinesis by the MEN and SIN. Trends Cell Biol 11, 89–95.

McCully EK, Robinow CF (1971). Mitosis in the fission yeast Schizosaccharomyces pombe: a comparative study with light and electron microscopy. J Cell Sci 9, 475–507.

Middendorp S, Kuntziger T, Abraham Y, Holmes S, Bordes N, Paintrand M, Paoletti A, Bornens M (2000). A role for centrin 3 in centrosome reproduction. J Cell Biol 148, 405–416.

Miron S, Durand D, Chilom C, Perez J, Craescu CT (2011). Binding of calcium, magnesium, and target peptides to Cdc31, the centrin of yeast Saccharomyces cerevisiae. Biochemistry 50, 6409–6422.

Moreno S, Klar A, Nurse P (1991). Molecular genetic analysis of fission yeast Schizosaccharomyces pombe. Methods Enzymol 194, 795–823.

Morrell JL, Tomlin GC, Rajagopalan S, Venkatram S, Feoktistova AS, Tasto JJ, Mehta S, Jennings JL, Link A, Balasubramanian MK, et al. (2004). Sid4p-Cdc11p assembles the septation initiation network and its regulators at the S. pombe SPB. Curr Biol 14, 579–584.

Moseley JB, Mayeux A, Paoletti A, Nurse P (2009). A spatial gradient coordinates cell size and mitotic entry in fission yeast. Nature 459, 857–860.

Mulvihill DP, Hyams JS (2002). Cytokinetic actomyosin ring formation and septation in fission yeast are dependent on the full recruitment of the polo-like kinase Plo1 to the spindle pole body and a functional spindle assembly checkpoint. J Cell Sci 115, 3575–3586.

Mulvihill DP, Petersen J, Ohkura H, Glover DM, Hagan IM (1999). Plo1 kinase recruitment to the spindle pole body and its role in cell division in Schizosaccharomyces pombe. Mol Biol Cell 10, 2771–2785.

Nigg EA, Raff JW (2009). Centrioles, centrosomes, and cilia in health and disease. Cell 139, 663–678.

Nigg EA, Stearns T (2011). The centrosome cycle: centriole biogenesis, duplication and inherent asymmetries. Nat Cell Biol 13, 1154–1160.

Nishikawa S, Terazawa Y, Nakayama T, Hirata A, Makio T, Endo T (2003). Nep98p is a component of the yeast spindle pole body and essential for nuclear division and fusion. J Biol Chem 278, 9938–9943.

Ohkura H, Hagan IM, Glover DM (1995). The conserved Schizosaccharomyces pombe kinase plo1, required to form a bipolar spindle, the actin ring, and septum, can drive septum formation in G1 and G2 cells. Genes Dev 9, 1059–1073.

Ohta M, Sato M, Yamamoto M (2012). Spindle pole body components are reorganized during fission yeast meiosis. Mol Biol Cell 23, 1799–1811.

Paoletti A, Bordes N, Haddad R, Schwartz CL, Chang F, Bornens M (2003). Fission yeast cdc31p is a component of the half-bridge and controls SPB duplication. Mol Biol Cell 14, 2793–2808.

Paoletti A, Moudjou M, Paintrand M, Salisbury JL, Bornens M (1996). Most of centrin in animal cells is not centrosome-associated and centrosomal centrin is confined to the distal lumen of centrioles. J Cell Sci 109, 3089–3102.

Peel N, Stevens NR, Basto R, Raff JW (2007). Overexpressing centriole-replication proteins in vivo induces centriole overduplication and de novo formation. Curr Biol 17, 834–843.

Pereira G, Schiebel E (2001). The role of the yeast spindle pole body and the mammalian centrosome in regulating late mitotic events. Curr Opin Cell Biol 13, 762–769.

Pérez-Mongiovi D, Beckhelling C, Chang P, Ford CC, Houliston E (2000). Nuclei and microtubule asters stimulate maturation/M phase promoting factor (MPF) activation in Xenopus eggs and egg cytoplasmic extracts. J Cell Biol 150, 963–974.

Piel M, Nordberg J, Euteneuer U, Bornens M (2001). Centrosome-dependent exit of cytokinesis in animal cells. Science 291, 1550–1553.

Pihan GA, Purohit A, Wallace J, Knecht H, Woda B, Quesenberry P, Doxsey SJ (1998). Centrosome defects and genetic instability in malignant tumors. Cancer Res 58, 3974–3985.

Reymond A, Schmidt S, Simanis V (1992). Mutations in the cdc10 start gene of Schizosaccharomyces pombe implicate the region of homology between cdc10 and SWI6 as important for p85cdc10 function. Mol Gen Genet 234, 449–456.

Robinow CF, Marak J (1966). A fiber apparatus in the nucleus of the yeast cell. J Cell Biol 29, 129–151.

Rodrigues-Martins A, Riparbelli M, Callaini G, Glover DM, Bettencourt-Dias M (2007). Revisiting the role of the mother centriole in centriole biogenesis. Science 316, 1046–1050.

Rose MD, Fink GR (1987). KAR1, a gene required for function of both intranuclear and extranuclear microtubules in yeast. Cell 48, 1047–1060.

Rosenberg JA, Tomlin GC, McDonald WH, Snydsman BE, Muller EG, Yates JR III, Gould KL (2006). Ppc89 links multiple proteins, including the septation initiation network, to the core of the fission yeast spindle-pole body. Mol Biol Cell 17, 3793–3805.

Salisbury JL (2007). A mechanistic view on the evolutionary origin for centrin-based control of centriole duplication. J Cell Physiol 213, 420–428.

Salisbury JL, Baron A, Surek B, Melkonian M (1984). Striated flagellar roots: isolation and partial characterization of a calcium-modulated contractile organelle. J Cell Biol 99, 962–970.

Salisbury JL, Suino KM, Busby R, Springett M (2002). Centrin-2 is required for centriole duplication in mammalian cells. Curr Biol 12, 1287–1292.

Sato M, Toya M, Toda T (2009). Visualization of fluorescence-tagged proteins in fission yeast: the analysis of mitotic spindle dynamics using GFP-tubulin under the native promoter. Methods Mol Biol 545, 185–203.

Selvapandiyan A, Kumar P, Morris JC, Salisbury JL, Wang CC, Nakhasi HL (2007). Centrin1 is required for organelle segregation and cytokinesis in Trypanosoma brucei. Mol Biol Cell 18, 3290–3301.

Sohrmann M, Schmidt S, Hagan I, Simanis V (1998). Asymmetric segregation on spindle poles of the Schizosaccharomyces pombe septum-inducing protein kinase Cdc7p. Genes Dev 12, 84–94.

Spang A, Courtney I, Fackler U, Matzner M, Schiebel E (1993). The calcium-binding protein cell division cycle 31 of Saccharomyces cerevisiae is a component of the half bridge of the spindle pole body. J Cell Biol 123, 405–416.

Spang A, Courtney I, Grein K, Matzner M, Schiebel E (1995). The Cdc31p-binding protein Kar1p is a component of the half bridge of the yeast spindle pole body. J Cell Biol 128, 863–877.

Stemm-Wolf AJ, Meehl JB, Winey M (2013). Sfr13 is a member of a large family of asymmetrically localized Sfi1-repeat proteins and is important for basal body separation and stability in Tetrahymena thermophila. J Cell Sci 126, 1659–1671.

Stemm-Wolf AJ, Morgan G, Giddings TH Jr, White EA, Marchione R, McDonald HB, Winey M (2005). Basal body duplication and maintenance require one member of the Tetrahymena thermophila centrin gene family. Mol Biol Cell 16, 3606–3619.

Tallada VA, Tanaka K, Yanagida M, Hagan IM (2009). The S. pombe mitotic regulator Cut12 promotes spindle pole body activation and integration into the nuclear envelope. J Cell Biol 185, 875–888.

Tanaka K, Kanbe T (1986). Mitosis in the fission yeast Schizosaccharomyces pombe as revealed by freeze-substitution electron microscopy. J Cell Sci 80, 253–268.

Tang X, Huang J, Padmanabhan A, Bakka K, Bao Y, Tan BY, Cande WZ, Balasubramanian MK (2011). Marker reconstitution mutagenesis: a simple and efficient reverse genetic approach. Yeast 28, 205–212.

Uzawa S, Li F, Jin Y, McDonald KL, Braunfeld MB, Agard DA, Cande WZ (2004). Spindle pole body duplication in fission yeast occurs at the G1/S boundary but maturation is blocked until exit from S by an event downstream of cdc10+. Mol Biol Cell 15, 5219–5230.

Vallen EA, Ho W, Winey M, Rose MD (1994). Genetic interactions between CDC31 and KAR1, two genes required for duplication of the microtubule organizing center in Saccharomyces cerevisiae. Genetics 137, 407–422.

Vonderfecht T, Cookson MW, Giddings TH Jr, Clarissa C, Winey M (2012). The two human centrin homologues have similar but distinct functions at Tetrahymena basal bodies. Mol Biol Cell 23, 4766–4777.

Weiss E, Winey M (1996). The Saccharomyces cerevisiae spindle pole body duplication gene MPS1 is part of a mitotic checkpoint. J Cell Biol 132, 111–123.

Winey M, Goetsch L, Baum P, Byers B (1991). MPS1 and MPS2: novel yeast genes defining distinct steps of spindle pole body duplication. J Cell Biol 114, 745–754.

Wu J-Q, Kuhn JR, Kovar DR, Pollard TD (2003). Spatial and temporal pathway for assembly and constriction of the contractile ring in fission yeast cytokinesis. Dev Cell 5, 723–734.

Wu J-Q, McCormick C, Pollard TD (2008). Counting proteins in living cells by quantitative fluorescence microscopy with internal standards. Methods Cell Biol 89, 253–273.

Wu J-Q, Pollard TD (2005). Counting cytokinesis proteins globally and locally in fission yeast. Science 310, 310–314.

Wu J-Q, Sirotkin V, Kovar DR, Lord M, Beltzner CC, Kuhn JR, Pollard TD (2006). Assembly of the cytokinetic contractile ring from a broad band of nodes in fission yeast. J Cell Biol 174, 391–402.

Yang CH, Kasbek C, Majumder S, Yusof AM, Fisk HA (2010). Mps1 phosphorylation sites regulate the function of centrin 2 in centriole assembly. Mol Biol Cell 21, 4361–4372.

Yang J, Liu X, Yue G, Adamian M, Bulgakov O, Li T (2002). Rootletin, a novel coiled-coil protein, is a structural component of the ciliary rootlet. J Cell Biol 159, 431–440.